Physics of Life Reviews 47 (2023) 211–244

Contents lists available at ScienceDirect

Physics of Life Reviews

journal homepage: www.elsevier.com/locate/plrev

Review

Control of movement of underwater swimmers: Animals, simulated animates and swimming robots

S.Yu. Gordleeva [a,b,c], I.A. Kastalskiy [a,c,*], Yu.A. Tsybina [a,d], A.V. Ermolaeva [a,d], A.E. Hramov [b,e], V.B. Kazantsev [a,b,c]

[a] National Research Lobachevsky State University of Nizhny Novgorod, 23 Gagarin Ave., Nizhny Novgorod, 603022, Russia
[b] Immanuel Kant Baltic Federal University, 14 A. Nevskogo St., Kaliningrad, 236016, Russia
[c] Moscow Institute of Physics and Technology, 9 Institutskiy Ln., Dolgoprudny, 141701, Moscow Region, Russia
[d] I.M. Sechenov First Moscow State Medical University (Sechenov University), 2 Bol'shaya Pirogovskaya St., Moscow, 119435, Russia
[e] Saint Petersburg State University, 7-9 Universitetskaya Emb., Saint Petersburg, 199034, Russia

ARTICLE INFO

Communicated by J. Fontanari

Keywords:
Fish locomotion
Central pattern generator
Spinal cord
Bio-inspired robotics
Swimming gait

ABSTRACT

The control of movement in living organisms represents a fundamental task that the brain has evolved to solve. One crucial aspect is how the nervous system organizes the transformation of sensory information into motor commands. These commands lead to muscle activation and subsequent animal movement, which can exhibit complex patterns. One example of such movement is locomotion, which involves the translation of the entire body through space. Central Pattern Generators (CPGs) are neuronal circuits that provide control signals for these movements. Compared to the intricate circuits found in the brain, CPGs can be simplified into networks of neurons that generate rhythmic activation, coordinating muscle movements. Since the 1990s, researchers have developed numerous models of locomotive circuits to simulate different types of animal movement, including walking, flying, and swimming. Initially, the primary goal of these studies was to construct biomimetic robots. However, it became apparent that simplified CPGs alone were not sufficient to replicate the diverse range of adaptive locomotive movements observed in living organisms. Factors such as sensory modulation, higher-level control, and cognitive components related to learning and memory needed to be considered. This necessitated the use of more complex, high-dimensional circuits, as well as novel materials and hardware, in both modeling and robotics. With advancements in high-power computing, artificial intelligence, big data processing, smart materials, and electronics, the possibility of designing a new generation of true bio-mimetic robots has emerged. These robots have the capability to imitate not only simple locomotion but also exhibit adaptive motor behavior and decision-making. This motivation serves as the foundation for the current review, which aims to analyze existing concepts and models of movement control systems. As an illustrative example, we focus on underwater movement and explore the fundamental biological concepts, as well as the mathematical and physical models that underlie locomotion and its various modulations.

* Corresponding author.
E-mail address: kastalskiy@neuro.nnov.ru (I.A. Kastalskiy).

https://doi.org/10.1016/j.plrev.2023.10.037
Received 27 October 2023; Accepted 29 October 2023

Available online 7 November 2023
1571-0645/© 2023 Elsevier B.V. All rights reserved.

Nomenclature

Acronyms

AHRS	attitude heading reference system
AI	artificial intelligence
AMPA	α-amino-3-hydroxy-5-methyl-4-isoxazole propionic acid-type glutamate
CIN	contralateral inhibitory neuron
CMOS	complementary metal oxide semiconductor
CNS	central nervous system
CPG	central pattern generator
DLR	diencephalic locomotor region
DMCU	decision mechanism-motion combination unit
DSP	digital signal processor
DTM	discrete time map
EDPU	environmental data processing unit
EIN	excitatory interneuron
ENS	electronic nervous system
GA	genetic algorithm
GABA	gamma-aminobutyric acid
GPS	global positioning system
I&F	integrate-and-fire
IINs	inhibitory interneurons
IMU	inertial measurement unit
IPSPs	inhibitory postsynaptic potentials
LIN	lateral inhibitory neurons
MLR	mesencephalic locomotor region
MN	motor neuron
NMDA	N-methyl-D-aspartate
nMLF	nucleus of the medial longitudinal fascicle
NOs	neural oscillators
ODEs	ordinary differential equations
PD	proportional-derivative
PID	proportional-integral-derivative
PNS	peripheral nervous system
RL	reinforcement learning
RS	reticulospinal
SN	sensory neuron
SNNs	spiking neural networks

1. Introduction

Motor control in living organisms represents one of the fundamental tasks that the brain has had to optimize for different creatures throughout evolution. In a general sense, motor control is organized by three main components: (i) neuronal circuits distributed in a hierarchical structure, (ii) the actuator system comprised of muscles, and (iii) a set of sensors that inform the control neuronal circuits about the environment and the current state of the actuators. The neuronal component can be further divided into lower-level subsystems typically located at the periphery, such as the spinal cord in vertebrates, and higher-level components in the central nervous system, such as the head and brain stem [8]. Spinal cord networks provide robust patterns of muscular activation that result in movement, while central nervous system (CNS) networks contribute to command-level control and fine-tuning. Locomotion represents a fundamental type of movement that involves the motion of the entire body in space. It is crucial for survival and, therefore, needs to be organized in a reliable and robust manner. Consequently, locomotion involves the repeated rhythmic activation of the body's strongest muscles. This activation is controlled by a relatively simple and robust neuronal circuit located in the spinal cord, known as the central pattern generators (CPGs) [94,63,3]. CPGs provide the basic type of animal movement in space, which can be realized without explicit command control or sensorial feedback. In critical situations, such as when an animal needs to escape, the central pattern generator (CPG) can work autonomously to generate locomotion patterns without requiring fine-tuning, energy optimization, or other higher-level modifications. On the other hand, higher-level control is organized in a more complex manner and is still an active topic of discussion in modern neuroscience [62,151].

The ability of animals to generate locomotion without relying on higher-level brain control has stimulated the design of biomimetic robots [125]. These robots imitate the bodies of animals and are driven by relatively simple and robust controllers that mimic the Central Pattern Generator (CPG). In many cases, these controllers are implemented using oscillatory electronic circuits that model motor neurons. These circuits have successfully tackled basic tasks involving robot movement in various conditions, including walking robots, flying robots, and swimming robots [142,208].

In the realm of autonomous motor control, swimming robots have become a focal point of interest for both fundamental scientists and engineering robotics. In comparison to other types of locomotion, the movement of underwater animals and corresponding robots does not involve the control of body position. Unlike walking creatures, swimming animals and robots do not need to maintain a specific "vertical pose" to prevent falling. In the case of flying animals, such as birds, gravity compensation is intricately linked to body translation in space. However, for water-dwelling creatures, the task of the CPG is solely focused on the locomotion of body translation in space. Furthermore, the aquatic medium is denser in comparison to air, which means that high-speed actuators, like those required for insect wings in the air, are not necessary for swimming control. Swimming can be more easily and reliably implemented in aquatic robots since it can operate at a slower pace.

Fishes, being aquatic creatures, rely on swimming as their fundamental mode of locomotion. In this review, we discuss the state-of-the-art concepts regarding the organization of fish swimming. We first explore the key aspects of motor control physiology, which encompass the features of fish body structure, actuators, brain and spinal cord organization, and the underlying CPG circuitry, including sensory feedback mechanisms. Additionally, we review mathematical models of CPGs, ranging from biophysically motivated neuronal circuits with feedback loops to more simplified oscillatory models used in the simulation of animate entities, such as virtual robots. These models also serve as a basis for engineering solutions aimed at controlling hardware robots for various types of aquatic locomotion.

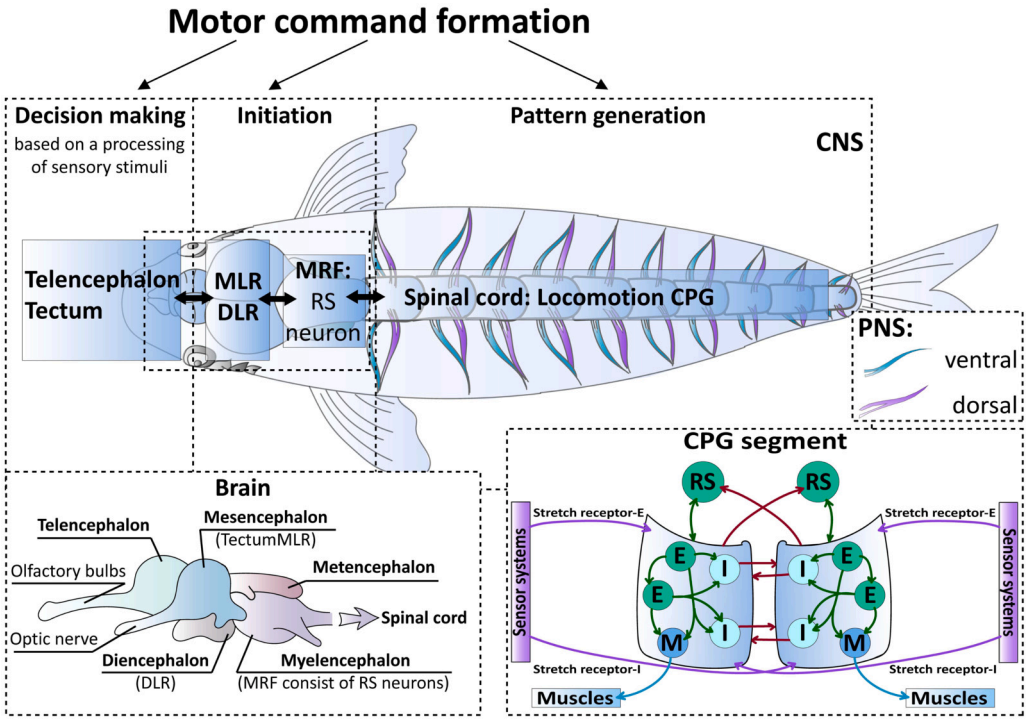

Fig. 1. Neural control structure for fish locomotion. Schematic representation of the brain, brainstem and spinal components that coordinate locomotor activity. Locomotion can be initiated by stimulating the diencephalic and mesencephalic locomotor regions (DLR, MLR), which receive input from the telencephalon and tectum. The DLR and MLR project excitatory signals to reticulospinal (RS) neurons, which then activate the spinal CPG responsible for generating rhythmic locomotor activity. The RS neurons excite all classes of CPG interneurons and motor neurons. The excitatory interneurons (E) stimulate all types of CPG neurons, including the inhibitory glycinergic interneurons (I) that cross the midline and inhibit all neuron types on the contralateral side, as well as the motor neurons (M). Sensory feedback to the CPG is provided by stretch receptor neurons. Two types of stretch receptor neurons exist: excitatory ones that activate ipsilateral CPG neurons, and inhibitory ones that suppress the activity of contralateral CPG neurons.

2. Neurobiology of fish locomotion system

In this section, we outline the conceptual framework of the fish motor system organization, including central networks, CPGs, and sensory control, focusing on one example from the lamprey. Due to its relative simplicity, the lamprey serves as a model of a swimming vertebrate nervous system and provides one of the few examples in which detailed knowledge about intrinsic organization of the spinal locomotor CPG networks is available. Since lampreys CPG is the most well-understood, it has been most modeled. For a comprehensive review of the cellular basis of motor behavior, we refer readers to Refs. [19,63,66].

Fish locomotion is controlled by the interplay between the central (CNS) and peripheral (PNS) nervous systems (Fig. 1). The CNS comprises the brain and spinal cord, which integrate and process information from the environment and control movements. The peripheral nervous system (PNS) includes the nerves that branch out from the brain and spinal cord, carrying sensory stimuli from the periphery to the CNS and motor commands from the CNS to the muscles [100,132]. In fish, the tectum, which is a part of midbrain, plays a central role in processing sensory information and generation of behavioral reactions. It integrates and coordinates different sensory modalities, such as visual, auditory, lateral line, somatosensory, and electrosensory, to provide a multimodal representation of the sensory environment [135]. Based on the received sensory input, the higher brain centers (the telencephalon and tectum) quickly make decisions to adjust behavioral movements to the dynamic environment. To initiate these movements, the higher brain centers send commands to the mesencephalic locomotor region (MLR) and diencephalic locomotor region (DLR). These two areas project independently to reticulospinal (RS) neurons in the middle and posterior reticulospinal nuclei, which in turn activate the spinal neural networks called the locomotor central pattern generators (CPGs) that generate locomotor activity [145,144,86,14,67,69]. The activation level of the locomotor regions defines the input signal to the spinal CPGs and therefore the locomotion speed.

The locomotion CPG is considered to be divided into segments according to the number of vertebrae. The spinal nerves originate from each vertebra, emerging from the ventral (abdominal) and dorsal (spinal) roots of the spinal cord. The ventral roots originate from motor cells located in the ventral horns of the spinal cord, and through these roots, excitation spreads to the periphery, activating the muscle fibers. The dorsal roots transmit sensory information from the fish's body to sensory neurons in the spinal cord, providing feedback. Thus, ventral roots contain motor nerve fibers, while dorsal roots contain sensory fibers. Fig. 1 illustrates the schematic interaction between the elements of the CNS and PNS that govern the control, initiation, and generation of swimming locomotion.

In the following sections, we will discuss in detail the roles of the main brain structures and spinal cord in fish motor control from a neurobiological perspective.

2.1. Fish brain

Movement control involves several brain structures such as telencephalon, mesencephalon (midbrain), diencephalon, metencephalon (cerebellum), and myelencephalon (medulla oblongata) (Fig. 1) [180]. The telencephalon, or forebrain, is involved in complex behaviors such as learning, memory and decision-making [100,132]. The midbrain is involved in motor control and processing of sensory information. The diencephalon integrates sensory information, controls hormone release, is related to regulating body temperature, hunger, and thirst. The cerebellum coordinates movement and balance. After muscle action has been initiated, the cerebellum governs the timing and coordination of muscle interactions [134]. The medulla oblongata regulates autonomic functions such as breathing, heart rate, and blood pressure [132,53].

In the midbrain, two subregions can be distinguished that are actively involved in the control of motor patterns: tectum and mesencephalic locomotor region (MLR) [146]. The tectum is the primary visual center in fishes and plays a central role in interfacing between sensory stimuli and behavioral reactions [24]. Situated dorsally in the midbrain, the tectum consists of two neuronal layers with specific cell types and connectivity. The superficial layer receives input from different sensory modalities (visual, auditory, lateral line somatosensory, electrosensory); and the deeper layer processes and integrates this information leading to a multimodal representation of the sensory environment in order to provide coherent orienting responses. Tectum, via its connections to premotor centers, controls eye movements, and behavioral motor patterns associated with survival and reproduction.

While tectum plays the main role in processing sensory stimuli, the MLR is believed to be a key brain region involved in goal-directed locomotion mainly due to its strategic location between higher brain centers and hindbrain neurons directly projecting to the spinal CPGs [126]. Located in the caudal mesencephalon the MLR receives signals from the higher brain structures, such as the telencephalon and tectum, in order to control locomotor initiation, locomotor speed and gait transitions (for recent review, [156,159,60]). Electrical stimulation of the MLR was able to elicit controlled swimming in lamprey [166], zebrafish [29], stingray [11] and salamander [25]. Wherein, the frequency of the movements and the force of muscle contractions were controlled by the stimulation strength.

Based on the processed sensory information the tectum via descending projections modulates the activity of the MLR neurons [52,161]. In particular, the tectum provides sensory feedback to the MLR about the orientation and movement of the fish in its environment, allowing the MLR to adjust its activity and generate appropriate motor outputs [70]. The exact nature of this feedback and the mechanisms by which it is integrated with other sensory and motor inputs in the MLR are still the subject of ongoing research [52]. Thus, the tectum and MLR work in tandem to generate adaptive locomotion in response to changes in the environment.

The exact organization and function of the MLR can vary between different species of fish and other lower vertebrates, and further research is needed to fully understand its role in locomotion control. The MLR consists of several nuclei, including the nucleus of the medial longitudinal fascicle (nMLF) and the adjacent area surrounding it [67,10]. These nuclei contain cholinergic and glutamatergic neurons. The glutamatergic neurons release glutamate, which activates the spinal cord neurons responsible for locomotion pattern generation. The inhibitory neurons release gamma-aminobutyric acid (GABA), which helps to fine-tune and coordinate the swimming movements by inhibiting some spinal cord neurons and exciting others.

When the MLR is activated, it generates a rhythmic pattern of neuronal activity that drives the swimming movements. The frequency and amplitude of this pattern can be modulated not only by signals from the higher-level brain regions, but also by sensory inputs received directly from the spinal cord and other sensory pathways, allowing the fish to adjust its ongoing motor activity to changing environmental conditions [4,16,136,159].

To control locomotion the MLR provides direct glutamatergic input to reticulospinal (RS) neurons in the medullary reticular formation (MRF)—as demonstrated in lamprey [14,143], zebrafish [29], salamander [157]. RS neurons in turn drive the interneurons of the locomotor CPG, as shown in lamprey [21]; for review, [66,107].

The mechanisms of the connections between the MLR and RS neurons has been extensively studied in lampreys [166]. Interestingly, it was shown that the strength of the connectivity between the MLR and RS cells posses the regional variation. Excitatory inputs from the MLR to RS cells are largest in those located in the rostral half of the hindbrain. As RS cells are situated further caudally, the strength of the inputs decreases. Additionally, stimulating RS cells with increased MLR strength follows a specific pattern, with cells located in the rostral hindbrain requiring the least amount of stimulation intensity, while those located more caudally require greater stimulation forces [14]. Thus, the MLR can activate different patterns of activity in the spinal cord to produce different types of swimming behaviors, such as forward swimming, turning, or escape responses [25,26,164].

In the diencephalon has been identified another region involved in controlling movement. The diencephalic locomotor region (DLR) is also involved in activating locomotion by providing the descending projection to neurons in the hindbrain. MLR and DLR project independently to RS neurons, which in turn activate the spinal CPGs that generate locomotor activity. Both pathways are glutamatergic and project bilaterally [1,195].

2.2. Fish spinal cord

The spinal cord is a long, tubular structure that runs along the length of the fish's body through the nerve channel of the spinal column and is protected by it. The spinal cord contains the neuronal networks that produce coordinated rhythmic patterns of motor neuron activity without receiving rhythmic inputs from sensory feedback or higher control centers. Such networks are referred to as CPGs. CPGs are distributed networks made up of multiple coupled oscillatory centers. The most basic CPGs underlie protective reflexes such as breathing, swallowing chewing, digesting, and coughing. Locomotion CPGs are activated by signals from RS neurons

of the brainstem locomotor center, which produces the locomotor pattern in close interaction with sensory feedback. With increased activation of the locomotor centers, the drive to the spinal locomotion CPGs increases, and therefore the locomotion speed increases.

In this section, we will describe the cellular bases of locomotion CPGs using the example of a lamprey's swimming CPG because it has been the most studied. The lamprey is a primitive eel-like fish and belongs to the class of lower vertebrates.

The lamprey nervous system can be considered a prototype for vertebrates, and it is convenient for neurophysiological study due to its simplicity and ability to be maintained in vitro. The isolated brainstem and spinal cord of lampreys can display normal electrophysiological properties and exhibit reflexes and swimming locomotion for several days. The lack of myelin in lampreys makes their brainstem and spinal cord relatively transparent, allowing for the visualization of nerve cell bodies and axons using a stereomicroscope. The spinal cord of the lamprey contains about 100 segments, with approximately 1000 nerve cells in each segment. Segmentation of the spinal cord is nominal and corresponds to the number of regularly occurring ventral and dorsal roots [19]. Since there is little apparent segmental organization beyond the nerve roots, and no distinctive clustering of nerve cells or their processes that would allow the recognition of segmental boundaries [149,150,162,174].

2.2.1. Locomotor rhythm generation by CPG

The lamprey's swimming pattern consists of rhythmic bursts of action potentials with a frequency ranging from 0.1 to 8–10 Hz in ventral roots that alternate between the left and right sides of the spinal cord. Each segment of the CPG represents a symmetrical oscillatory center responsible for the movement of a specific body part [30,63,52]. The core of the lamprey CPG network is formed by ipsilateral glutamatergic excitatory interneurons (EIN in Fig. 1), glycinergic inhibitory interneurons (IIN in Fig. 1) with contralateral axons, and motor neurons (MN in Fig. 1). In a single CPG hemisegment, the rhythmic bursts are generated by the activity of the ipsilateral excitatory interneuron population. The excitatory interneurons release glutamate that activates α-amino-3-hydroxy-5-methyl-4-isoxazole propionic acid-type glutamate (AMPA) and N-methyl-D-aspartate (NMDA) receptors on postsynapses of all spinal neuron types. They excite not only nearby excitatory interneurons and ipsilateral motor neurons, but also the glycinergic inhibitory neurons, whose axons cross the midline to inhibit all neuron types on the contralateral side [61,119,18,121]. There are two types of neurons that are involved in crossed inhibition. The first type is made up of larger neurons which have long descending axons. The second type is made up of smaller interneurons which have much shorter axons. These smaller interneurons provide larger inhibitory signals, known as unitary inhibitory postsynaptic potentials (IPSPs), compared to the larger neurons [138]. In addition to these two main types of neurons, there are also small glycinergic interneurons that are activated alongside motor neurons, likely by excitatory interneurons. These glycinergic interneurons provide monosynaptic inhibition to both motor neurons and crossed inhibitory interneurons (IINs) [138,22]. Glycinergic 'lateral interneurons' have a large cell body, prominent lateral dendrites, and fast-conducting, long ipsilateral axons projected caudally. They locate rostrally in the spinal cord and probably subserve mainly a propriospinal function.

RS glutamatergic neurons drive the CPG network by activating AMPA and NMDA receptors on motor neurons, excitatory interneurons and crossed inhibitory interneurons. The voltage-dependent NMDA receptors induce the plateau-like depolarizations of the neurons that play a key role in the generation of long-lasting bursts and a slow, regular locomotor activity.

2.2.2. Sensory feedback to the CPG

The sensory feedback to the CPG is provided by stretch receptor neurons, also known as edge cells. They have a dendritic tuft that mediates stretch transduction. During each swim cycle, lateral bending movements are detected by stretch receptors located at the lateral margin of the spinal cord. As the muscle fibers in one hemisegment contract, the stretch receptors on the opposite side are extended. There are two types of stretch receptor neurons: inhibitory glycinergic stretch receptor neurons with contralateral axon projection that terminate the activity of the contralateral CPG neurons (on the side that is actively contracted), and excitatory glutamatergic stretch receptor neurons that excite the ipsilateral CPG neurons, which become active after the cessation of activity on the opposite side. This sensory input is strong enough to synchronize the rhythmic activation of the stretch receptor neurons with the CPG-produced locomotor rhythm through alternating movements. Several experiments have shown the crucial role of sensory feedback in shaping CPG activity. It has been demonstrated that mechanically moving the lamprey's tail induces the generation of a CPG rhythm that is frequency-locked with the stimulation frequency.

In the lamprey spinal cord, the dorsal cells are primary mechanosensory neurons that respond to skin touch [36,130]. They are classified into two types: touch and pressure cells [120,34,35]. These cells participate in local reflexes and are activated during lamprey's fictive swimming caused by electrical stimulation [17,23,1,117,7].

2.2.3. Intersegmental coordination

Swimming vertebrates such as lamprey, fish, salamanders swim by producing a mechanical undulatory wave that propagates along its body and pushes it forward through the water. This movement is generated due to the delay between the activation of consecutive segments along the spinal cord (Fig. 2). This phase lag remains constant and is equal a certain proportion of the cycle duration. As it has been shown in most fish species, standard coordination during swimming requires that the phase lag between the most rostral and the most caudal segments is always constant, usually around 100% of cycle duration. The phase lag can be modulated by sensory signals that directly come to spinal cord. Experiments with isolated spinal cord have revealed that the generation of a constant phase lag between segments is an inherent feature of spinal cords, both in the case of forward locomotion when the rostral segments lead with a constant rostro-caudal phase lag and for backward locomotion when the phase lag is reversed into a caudo-rostral lag. Such intersegmental coordination on the cellular level is organized by connectivity of excitatory interneurons, which extend their axons over a few rostral and a greater number of caudal segments.

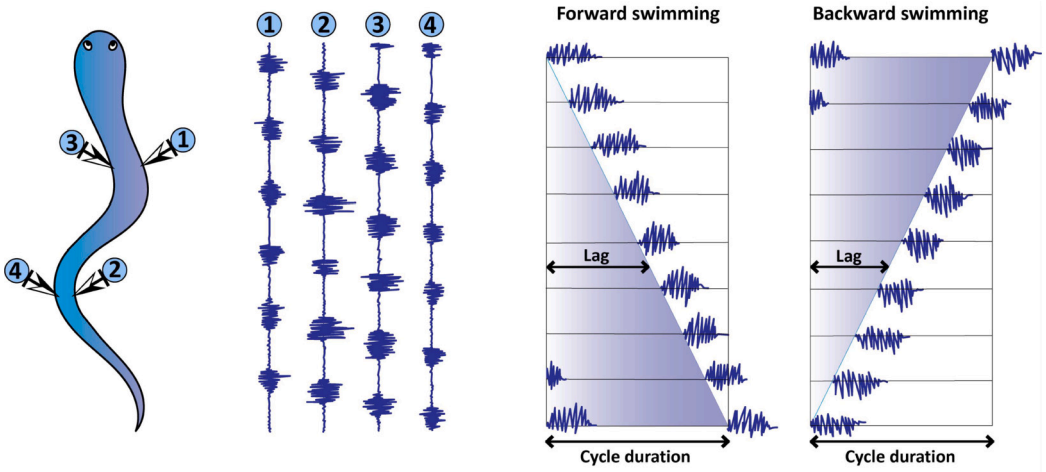

Fig. 2. The lamprey swims by propagating a mechanical wave, transmitted along the body. Consecutive segments of the spinal cord are activated with a phase lag that is a fixed proportion of the cycle duration. Source: adapted from [63].

2.2.4. Steering

Forward locomotor activity is induced by symmetrical bilateral activation of the RS neurons. Asymmetrical activation results in left-right turning [124,57,46]. Greater activation of RS neurons on one side leads to the generation of longer bursts on ventral roots on this side, causing the movement direction to shift towards that side. Similarly, vertical deviations are caused by asymmetric activation of ventral or dorsal myotome neurons by RS neurons. Head movements are induced by vestibular input through interneurons on contralateral RS neurons. Left-right turning of the head results in asymmetric activation of the RS neurons, producing an automatic correction of body orientation [44,45]. The vestibular input plays a major role in postural control for fish.

3. Locomotion CPG models

While knowledge of the various neural networks present in the lamprey motor system, including their interneuron connectivity, types of synaptic transmission, and subcellular properties, is essential for understanding CPGs, it is not sufficient on its own. The dynamics of interactions, spanning from molecular to network levels, are highly complex. Therefore, computational approaches are necessary to investigate whether intuitive explanations can account for experimental findings. In the section, we will attempt to review all of the basic models that are used to build and simulate a CPG of the fishes and swimming animals, such as turtles or salamanders, moving from the simple to the complex. Fig. 3 illustrates the hierarchy of models used in the fishes's CPGs development, while being the outline of our review.

It should also be noted that the problem of creating CPGs based on coupled nonlinear oscillating elements exhibiting complex patterns of collective dynamics has a close connection with the problems of signal propagation in complex networks, which has been recently addressed in the reviews [87,88]. In this context, we can consider the problem of constructing CPGs from both modeling-driven approaches and data-driven methods. Following the first approach, knowing the required motion patterns of body segments of a swimming organism or a swimming robot, we can, based on the interplay between the structure of connections between oscillators and their dynamics, try to form the required motion pattern. We can even optimize the motion pattern with this approach by changing the configuration and strength of the links between oscillatory nodes, for example, to achieve the maximum swimming speed. Such a modeling-driven method is conveniently applied using abstract oscillatory models known from nonlinear dynamics to design CPGs of swimming robots. The second data-driven approach appears to be an inverse problem for identifying the hidden biological features of real fish or waterfowl animal CPGs from known biological data. This approach allows us to construct biologically plausible models of CPGs that describe the organization of neural networks of different fish species. We then consider these issues related to the CPGs model classification in more detail in Section 3.1.

3.1. CPG models classification

CPG models are typically constructed as systems of interconnected segments, each exhibiting specific collective dynamics. The architecture of a CPG model enables the establishment of the desired pattern of rhythmic activity, corresponding to the movement of different body parts in swimming animals or the moving components of floating robots (if we consider artificial objects rather than biological ones). The topology of CPG model architectures can be highly diverse, but the most commonly employed structures include one-dimensional (1D) chains, two-dimensional (2D) lattices, and network-like (3D) arrangements of CPG segments.

The simplest CPG models consist of 1D chains of connected segments, where each segment is linked to its two nearest neighbors. This topology is often used to simulate CPGs involved in basic locomotion behaviors, such as swimming forward. In contrast, a 2D topology refers to a lattice-like organization of segments, where each segment is connected to its three closest neighbors. This topology is frequently utilized to model CPGs responsible for more complex behaviors, which involve the processing of external

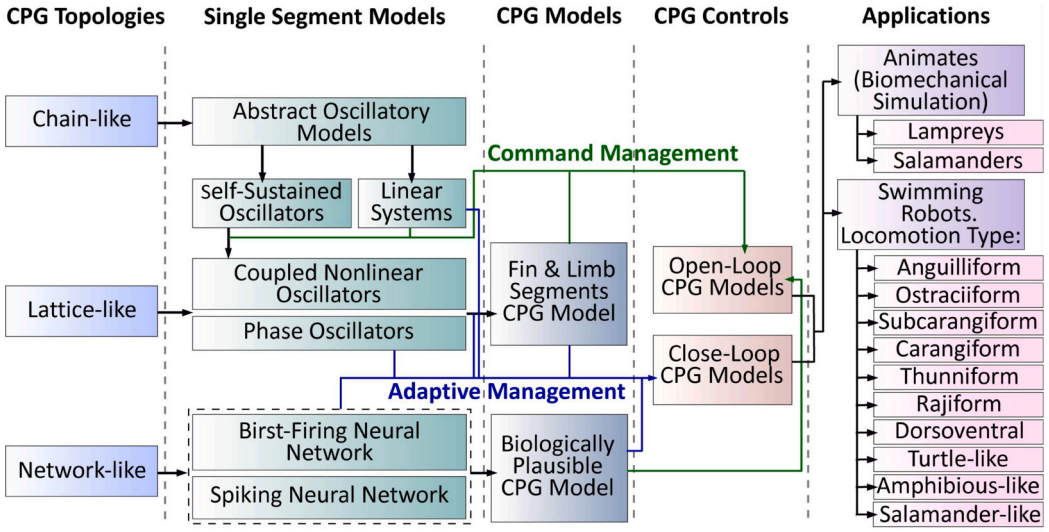

Fig. 3. A hierarchy of CPG models for floating animals and their development to create CPGs for floating robots that are considered in the review.

sensory information to perform adaptive actions like obstacle avoidance or prey capture. A network of segments represents an even more intricate 3D structure, where each segment is connected to a larger number of neighbors. The arrangement of segments in these complex networks is defined by an adjacency matrix and described in terms of graph theory. The wide range of dynamics exhibited in such complex networks allows for a vast variety of dynamic and synchronous modes to be realized. Furthermore, these networks can be utilized to create biologically plausible models of CPGs.

The paper [133] compares the performance of the three CPG topologies in terms of their ability to generate stable and coordinated motion, their resilience to disturbances and perturbations, and their computational efficiency. The results of the study demonstrate that the 3D CPG topology outperforms the other two topologies in terms of stability, reliability, and efficiency. The 3D topology is able to produce coordinated motion with minimal intersegmental coupling, making it more robust to disturbances and easier to control. Niu et al. [133] conclude that the 3D CPG topology is a promising approach for controlling the locomotion of underwater vehicles and could have potential applications in areas such as marine exploration, underwater robotics, and biomimetic locomotion. However, for the construction of simple CPGs for technical robotic applications this complexity and richness of oscillatory modes looks redundant, so simpler 1D and 2D topologies remain also very much in demand in practice.

It should be noted that the CPG segments themselves may have different intrinsic dynamics and may be described by different mathematical models. The corresponding segment models can be both abstract models that is unrelated to the biological context but demonstrates the necessary dynamics. In this case, the most commonly used models are models of self-sustained oscillators with limit cycles (see Section 3.2) those oscillatory modes do not depend on initial conditions (in the absence of multistability [139]]) and whose characteristics (primarily frequency and phase of oscillations) can be controlled within certain limits by external signals due to the effect of synchronization. There are also works [188,193] that use linear differential equations as the mathematical models of the CPG segment. For a more flexible adjustment of the dynamics of such segments, it is convenient to use coupled oscillators [83,84,98,204,104], which have wider possibilities for controlling the phase characteristics of oscillations in them by fine-tuning the parameters of coupled systems or communication channels between them.

More advanced models already have a biologically plausible form and include various mathematical models of connected neurons organised into neural ensembles, both birst-firing and spiking neural networks [12,111,113,81,9,75,98] (see Section 3.3). Such models approximate those real CPGs that are implemented by nature in the different fish species. We specifically focus in the Section 3.4 on the biophysically detailed, full-scale computational model of the fish CPG and its forebrain control [101], which was one of the first fully realistic models based on biophysical data of the lamprey locomotor CPG. Two other biologically relevant CPG models of the brainstem-spinal cord network in lampreys [102] and a detailed model of the complete neuronal circuit of frog tadpoles [58] are also reviewed in the Section 3.4. In the latter, the role of the interplay between receiving sensory signals, decision making, and locomotion generation in the operation of CPGs was considered. Such models offer significant opportunities to study the biophysical mechanisms of locomotion rhythm generation in the central and peripheral nervous system of swimming animals. However, for use in applied robotic tasks, such the models prove to be too complex and poorly controllable in terms of the need for closed-loop control systems. In the closed-loop CPGs, sensory information and the commands generated from its processing influence the dynamics of CPGs, self-consistently changing the rhythm and pattern of robot movement depending on the external environment and commands to change the direction of the swimming robot. Models that include additional segments for self-consistent description of fin and limb movements also belong to such the systems.

Therefore, to develop models of CPGs that can be applied in robotics tasks for creating either simulated biomechanical models (animates) or floating robots, it is necessary to base the models on the simpler models with 1D or 2D topologies. In robotics tasks, simple abstract oscillatory models, which are much easier to implement and program, are often used as model systems in individual

segments of CPGs. Such models have now been developed for virtually all types of fish and waterfowl locomotion. We also discuss these in our review in Section 4.3.

3.2. Abstract ODE-based oscillator models

The simplest and most common approach to modeling CPGs is to use systems of coupled oscillators described by the ordinary differential equations (ODEs). In these models, the activity of a neural population in a complete CPG segment is represented by an oscillator, rather than a single neuron or a small circuit. Nonlinear oscillators are employed to describe nonlinear dynamics, which may not be bioinspired or biologically meaningful, unlike neural oscillators (NOs) that typically have clear biological meanings. Nonlinear oscillators commonly exhibit self-sustained limit cycle generation and selective entrainment. As swimming of fish can be characterized by rhythmic patterns, nonlinear oscillators would be an ideal tool to control the swimming motion [221].

The purpose of these models is not to explain rhythmogenesis, as oscillatory mechanisms are assumed to already exist. Instead, the models aim to investigate how inter-oscillator couplings and differences in intrinsic frequencies affect the synchronization and phase lags within a population of oscillatory centers. This modeling approach is motivated by the fact that the dynamics of populations of oscillatory centers primarily depend on the type and topology of couplings, rather than the local mechanisms of rhythm generation, which are well-established in dynamical systems theory. In biophysics, a key to understand the rhythm generation is the concept of the half-center (or bipartite) model proposed in [15] and refined in [170]. According to this concept, the rhythmic pattern of alternating bursts of flexor and extensor activities is produced by two symmetrically organized excitatory neural populations that drive alternating activity of flexor and extensor motoneurons and reciprocally inhibit each other via inhibitory interneurons. The oscillator model is based on the assumption that the CPG segment consists of two populations of neurons that mutually inhibit each other. When one population is active, it inhibits the other, causing it to become inactive. This, in turn, allows the first population to become active again. The activity of the two populations of neurons can be described by two variables that represent the strength of their respective inhibitory connections. The dynamics of the system can be described by a set of ODEs that govern the evolution of these variables.

The self-sustained oscillators are often used for modeling and engineering of fish CPGs because they are simple, easy to analyze and can produce complex and flexible patterns of activity. Such models have the capability to generate a wide range of output patterns, including irregular and chaotic activity. For instance, self-sustained oscillators can produce asymmetrical or irregular swimming patterns, which are commonly observed in fish that navigate complex environments or engage in complex social interactions [21]. They can also respond to changing sensory inputs and modulatory signals by adjusting their output patterns in real time. This flexibility is crucial for fish that need to navigate dynamic and unpredictable environments, where they may encounter obstacles, predators, or prey [82]. Another advantage of ODE-based models is their ability to generate multiple output patterns from a single oscillator. For example, Zhou and Low [221] shown that the use of Hopf oscillators as the segments of CPG makes it possible to realise a quick transition of the motion pattern during the online tuning of the controlling parameters. Another approach here is incorporating nonlinear feedback loops or coupling multiple oscillators together, enabling the system to generate a wider range of behaviors with fewer components [56,73].

3.2.1. Hopf oscillator-based CPG model

Let us take a look at a few popular and widely used individual segment oscillatory models for CPG development. One of the popular nonlinear oscillator models used in development of CPGs is the Hopf oscillator. First, the rhythmic output pattern of Hopf oscillator has a clear relationship with its parameters that facilitate the easy shaping of the output pattern by modulating corresponding parameters. Second, it is easier to develop coupling terms for multiple coupled Hopf oscillators in which the phase difference between the oscillators can be arbitrarily chosen [198]. The coupled Hopf oscillators dynamics is illustrated in Fig. 4A and is described by the following ODEs [221]:

$$\dot{\mathbf{X}}_i = F(\mathbf{X}_i) + \mathbf{C}_i = \begin{pmatrix} \left(\rho^2 - \left(u_i^2 + v_i^2\right)\right) u_i - \omega v_i, \\ \left(\rho^2 - \left(u_i^2 + v_i^2\right)\right) v_i + \omega u_i, \end{pmatrix} + \begin{pmatrix} c_{u,i}, \\ c_{v,i}, \end{pmatrix}, \tag{1}$$

where $F(\mathbf{X}_i)$ is the nonlinear operator defined by the Hopf oscillator, the state vector in Cartesian space are represented by $\mathbf{X}_i = (u_i, v_i)^T$, the coupling term is determined by a coupling vector $(c_{u,i}, c_{v,i})^T$), the amplitude of the oscillation is controlled by positive number ρ, and ω is the intrinsic oscillation frequency. The steady-state outputs of the single Hopf oscillator with $\mathbf{C} = 0$ produces harmonic-like oscillations u and v that can be illustrated by Fig. 4B. The only attractor of Hopf oscillator is its limit cycle, as shown in Fig. 4B. When the evolution starts from different initial conditions (states 1–8), the Hopf system state always asymptotically converge to a limit cycle with radius A as time increases.

Usually, the Eq. (1) are considered as a chain of oscillators with different coupling vectors $\mathbf{C}_i$ depending on the problem to be solved. In particular, in Refs. [221,222] considered a model of CPGs with a chain structure and mutual couplings as shown in Fig. 4A) where $c_{u,i} = 0$, $c_{v,i} = \varepsilon(u_{i-1}\sin\varphi_i - u_i\sin\varphi_{i+1} + v_{i-1}\cos\varphi_i - v_i\cos\varphi_{i+1})$. In this case, the control signal of each oscillator is written as

$$\Theta_i = A_i u_i, \tag{2}$$

where A_i is the amplitude of each segment oscillations. It is common to impose constraints on the amplitudes of all segments due to the fact that the waveform of a live fish with an elongated propulsion shape usually has gradually increasing amplitudes from head

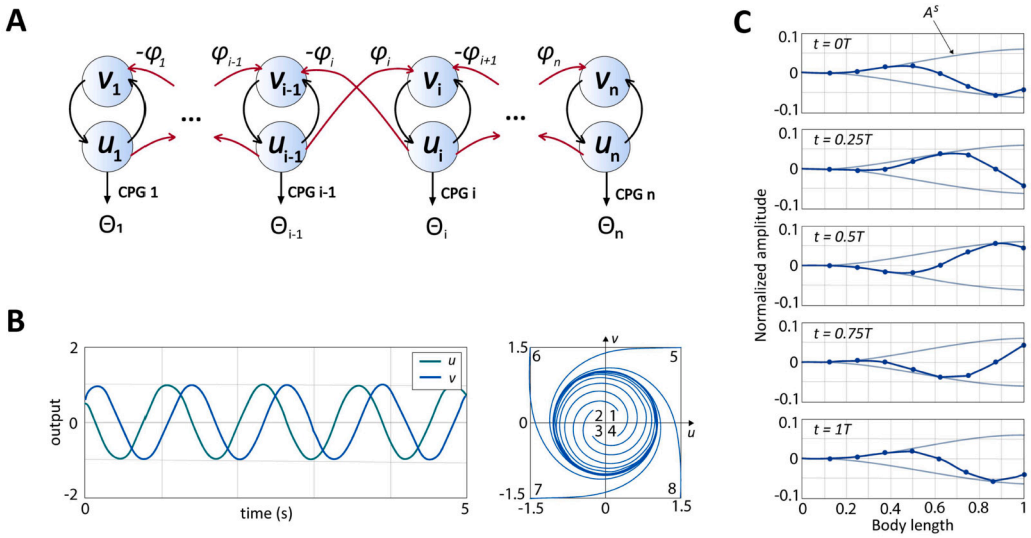

Fig. 4. CPG based on the Hopf oscillator. (A) Structure of CPGs with a chain structure and mutual couplings. (B) Oscillations and limit cycle of the single Hopf oscillator ($\mathbf{C} = 0$). (C) Examples of optimal profiles of control signal amplitude A_i at different times in one undulation cycle associated to the optimal speed. Sources: adapted from [222] (panels A and C) and [221] (panels A and B).

to tail [93]. The shape of body motion is believed to be related to high energy efficiency of swimming [179]. The constraint can be simply defined as follows

$$0 \le A_1 \le \cdots \le A_{i-1} \le A_i \le \cdots \le A_n, \tag{3}$$

where A_n is characterized by the upper amplitude, which is decided by the maximum power of actuators. The specific parameters of the amplitudes A_i are determined as a result of one or another CPG optimization, for example, the shape of the profile $A_i = A(i\Delta x)$ may be determined by the condition of achieving the maximum fish speed, where Δ_x is the spatial pitch of the fish segments, each of which is controlled by its own Hopf generator. In Ref. [222], the optimization was performed using a genetic algorithm and the optimal waveform associated with the maximum speed was found $A^S(x) = -0.1323x^3 + 0.2125x^2 - 0.0194x - 0.0001656$. Fig. 4C shows examples of optimal profiles generated by the CPG (1) and ((2) at different times in one undulation cycle. Numerous experimental and numerical simulation studies on robotic fish have shown that CPGs based on Hopf oscillators exhibit high stability, controllability and feasibility in the form of electronic circuits for robot control robots [222,198,200,213,190,78,221,218,212,110,163,220].

3.2.2. *Matsuoka oscillator-based CPG model*

Another widely used model for CPG segment dynamic is the Matsuoka oscillator [122,123]. Matsuoka has studied the self-sustained oscillations generated by mutually inhibiting neurons with adaptation, and has discovered some of the mechanisms of frequency and pattern control in the neural rhythm generators. The Matsuoka oscillator describes a pair of mutually inhibiting neuron oscillators (NOs) as shown in Fig. 5A and is represented by:

$$\begin{aligned} T_r \dot{x}_i &= -x_i - b f_i - \sum_{j=1}^{n} a_{ij} y_j - \mathcal{F}_i + s_i, \\ y_i &= g(x_i) = \max(0, x_i), \\ T_a \dot{f}_i &= -f_i + y_i, \end{aligned} \tag{4}$$

where $n = 2$, x_i is a neuronal membrane potential, f_i is the variable that represents the level of neuronal adaptation or fatigue and a_{ij} (≥ 0 for $i \neq j$ and $= 0$ for $i = j$) is a weight for inhibitory synaptic connection from the j-th neuron to the i-th neuron. An impulse "rate" of the tonic or slowly varying input is given by s_i and y_i represents output of the neuron or firing rate. The parameter b specifies the steady-state firing rate for a constant input. T_r and T_a represent a time constants for the rise time and the adaptation time lag, respectively. Additionally, $\mathcal{F}_i$ corresponds to feedback signal from the robot. Fig. 5B demonstrates oscillations generated by cyclic inhibition networks consisting of two neurons without any feedback $\mathcal{F}_i = 0$. All NOs of a network receive the same magnitude of excitatory stimuli from the outside of the network $s_i = 1$ ($i = 1, 2$), and inhibitory stimuli from the inside neurons. Excited oscillations are periodic and occur in counter-phase on both neurons.

The Matsuoka model is of particular interest due to the possibility of realising sensorimotor feedback and, consequently, controlling the CPGs in an unpredictable environment. In Ref. [172,71] the bipedal and quadrupedal locomotion of a robot was considered. It was shown that stable and flexible locomotion is realised as a limit cycle generated by the global coordination of the rhythmic activity of the nervous system, consisting of coupled neural oscillators, and the rhythmic movements of the locomotor apparatus involving interaction with the environment. Coordinated movements are formed not by explicitly representing the exact movement

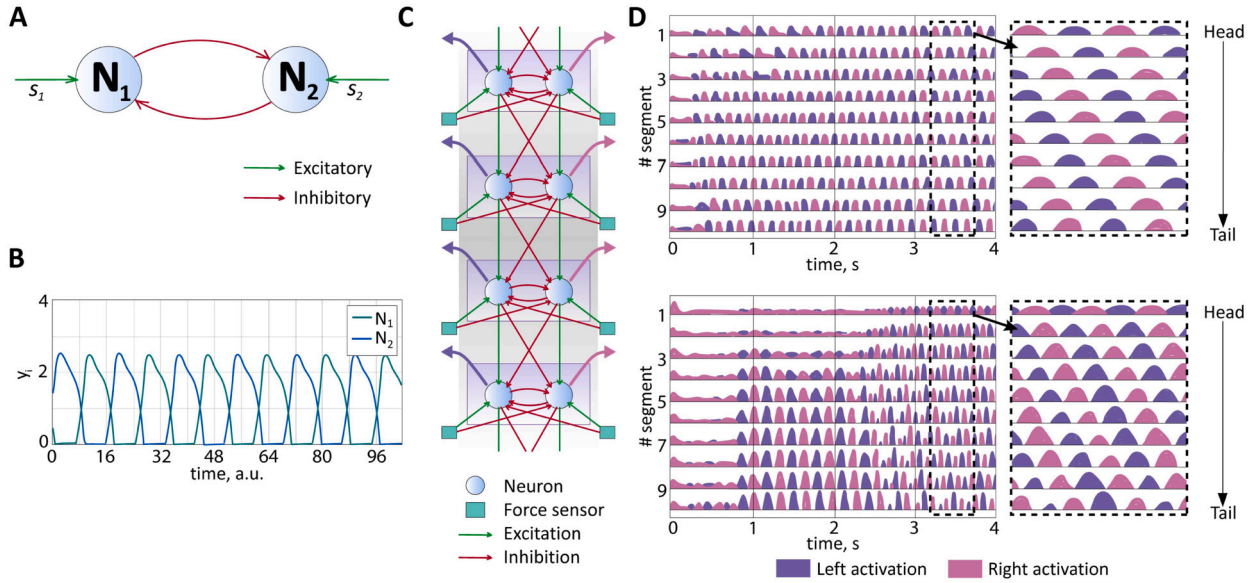

Fig. 5. CPG based on the Matsuoka NO. (A) The Matsuoka model with two mutually inhibiting NOs. (B) The rhythmic activity of Matsuoka model consisting of two neurons. Parameters $T = 12$, $a = 2.5$, and $b = 2.5$. Excited oscillations are periodic and occur in counter-phase on both neurons. (C) General structure of CPG based on Matsuoka neural network model with force sensors. (D) Spatio-temporal oscillations showing the emergence of a rostral-caudal traveling wave in the output of the NOs of the left and right sides that is sent as activation to the muscles in the case of the decoupled configuration with removing intersegmental coupling of CPGs NO (top) and the oscillator-free configuration with removing the mutual inhibition within segments of CPG (bottom). Sources: adapted from [122] (panels A and B) and [175] (panels C and D).

trajectories of each part, but by the dynamic interaction between the nervous system, musculoskeletal system and the environment. Stepping movements that are robust to mechanical perturbations and environmental changes were obtained. Moreover, the Matsuoka model generated not only walking movements but also the running movement by changing a single parameter nonspecific to the movement.

Due to this feature, the Matsuoka model (4) has also been used in swimming locomotion systems to study locomotion control during swimming [175,79]. In [175], undulatory swimming is considered as a model for studying locomotion control during self-organized swimming. Many vertebrate swimmers have CPGs and local pressure-sensitive receptors that provide information about the surrounding fluid. The authors [175] used a specially designed robot that transmits the basic components of the animal's neuromechanical system and numerical simulation of Matsuoka model (4) based CPG to investigate the sensed hydrodynamic pressure forces can control body movements through local feedback loops. Fig. 5C illustrates a CPG model based on a modified Matsuoko NOs with feedback from left and right force sensors that controls the motion of a robot with undulatory motion. Two simpler configurations were considered: (i) the decoupled configuration implemented by removing intersegmental coupling, and (ii) the oscillator-free configuration was explored by removing the mutual inhibition within segments. Fig. 5 D shows the dynamics of activation of left and right neurons corresponding to the traveling waves of body undulations emerging thus showing that the t neural couplings from the force-sensing neurons can successfully entrain neural activation to obtain needed swimming locomotion.

3.2.3. Coupled oscillators as CPG model

Using a pair of oscillators as a CPG segment is also very effective for the formation of movement patterns of swimming animals. Very often in this case, coupled phase oscillators are used, which allow, by controlling their amplitude and coupling, to realise various rhythmic patterns, including even switching between activity types. In particular, in Ref. [84], Ijspeert et al. proposed a CPG model describing fast switching between two locomotion modes: swimming and walking on the example of a salamander robot. This model had a significant impact on such studies and later this model and its various modifications have been used in a large number of studies as a CPG model [42,116,43,105,211,191,201,32,203,41,49,48,207].

Ijspeert et al. used a pair of coupled phase oscillators as the salamander CPG segment: one for left and one for the right side of the body [84]. The oscillators in the model have a phase-resetting property, which allowed the model to adapt to different conditions and generate a wide range of locomotion patterns from swimming to walking. Configuration of the CPG model is shown in Fig. 6A. The model is composed of 20 amplitude-controlled phase oscillators and can be divided on two parts. First, it is a body CPG including a double chain of 16 oscillators with nearest-neighbor coupling for driving the spine motors. Second, it is a limb CPG corresponding to 4 oscillators for driving the limb motors. The bursting properties of an oscillatory center, in other words the oscillations between bursts of motoneuron activity and periods of rest, are modeled by means of a phase oscillator with controlled amplitude

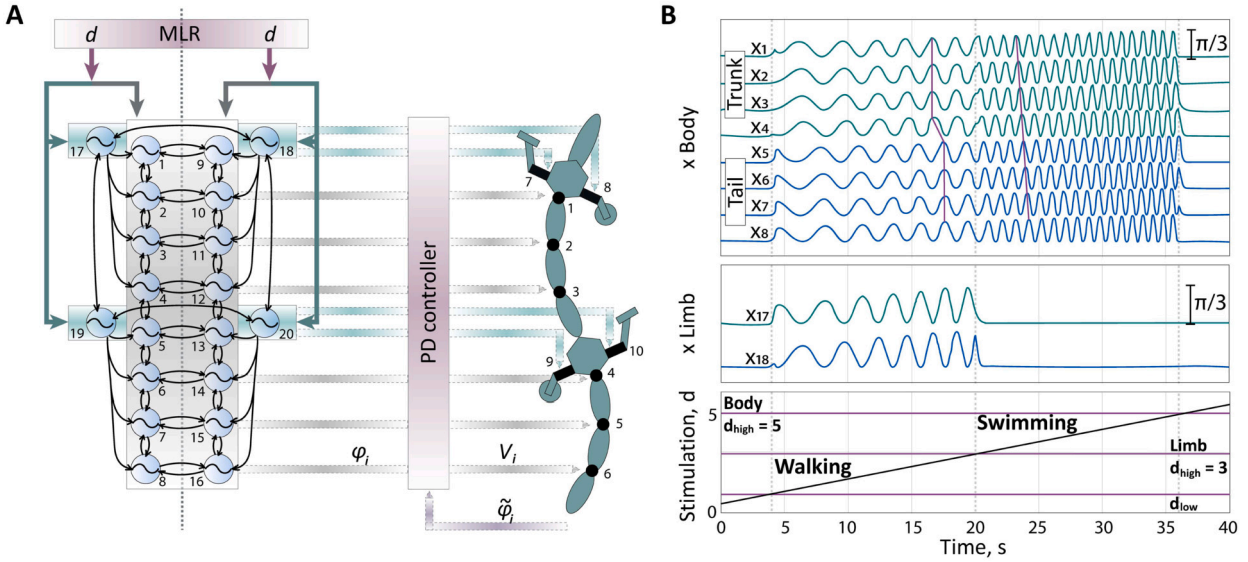

Fig. 6. (A) Configuration of the CPG model based on coupled phase oscillators and schematical representation of a salamander robot under the CPG control. (B) Gait transition from walking to swimming with the salamander CPG model: (top) output signals from the left body CPG oscillators (phase oscillators of body and limbs on the right side demonstrate anti-phase oscillations). The red lines illustrate the transition from standing waves (with synchrony in the trunk, synchrony in the tail, and an anti-phase relation between the two) to traveling waves. (medium) output signals from the left limb CPG oscillators. (bottom) Linear increase of the stimulation signal applied to all oscillators. Source: adapted from [84].

$$\begin{aligned}\dot{\theta}_i &= \omega_i + \sum_j r_j w_{ij} \sin(\theta_j - \theta_i - \phi_{ij}),\\ \ddot{r}_i &= a_i^2(R_i - r_i)/4 - a_i \dot{r}_i,\\ x_i &= r_i(1 + \cos(\theta_i)),\end{aligned} \tag{5}$$

where the state variables θ_i and r_i represent the phase and the amplitude of oscillator i, ω_i and R_i denote its intrinsic circle frequency and amplitude, respectively. a_i is a positive constant determining how quickly the variable r_i converges to R_i. The weights w_{ij} and phase biases ϕ_{ij} define the couplings between oscillators. x_i is a positive oscillatory signal that represent the burst produced by the center.

The chain of oscillators receive a drive signal representing the descending stimulation from the MLR in the brainstem. The outputs of the CPG are desired joint angle positions φ_i that are used by a proportional-derivative (PD) feedback controller (V_i are the voltages applied to the motors and $\tilde{\varphi}_i$ are the actual joint angles measured from incremental encoders as shown in Fig. 6A). Tuning the parameters of such a model is a complex process and involves a number of assumptions about the dynamics of the CPG of living organisms. (i) The body CPG is like that of the lamprey and spontaneously produces traveling waves when activated with a continuous stimulation. The limb CPG, when activated, forces the whole CPG into the walking mode [37]. (ii) The strengths of the couplings from limb to body phase oscillators are stronger than those from body to body phase oscillators and from body to limb phase oscillators. This allows the limb CPG to switch the mode of operation of the body CPG from traveling wave generation to standing wave production if necessary. (iii) Under the same stimulation, limb oscillators have lower intrinsic frequencies than the body oscillators. Limb oscillators cannot oscillate at high frequencies, that is, they saturate and stop oscillating at high levels of stimulation. This provides a mechanism for automatically switching between walking and swimming when the stimulation from brain is varied [25] and explains why swimming frequencies are systematically higher than walking frequencies [59,47]. Finally, it is known [25,65] that in the swimming animals, the amplitude and frequency of bursts depend on the amount of stimulation. Therefore, depending on the intensity of stimulation we can talk about three modes of CPG: (i) a subthreshold phase without bursts; (ii) an oscillating phase where the frequency and amplitude of bursts increase with the stimulation intensity; and (iii) a saturation phase where centers stop oscillating. This can be described mathematically by introducing a piecewise linear saturation function, which similarly modulates the intrinsic frequency ν_i and amplitude R_i according to a stimulation signal d between a lower oscillation threshold, d_{low}, and an upper one for limb, d_{high}^{limb}, and body, d_{high}^{body}. Limb and body oscillators are provided with different saturation functions, with the limb oscillators systematically oscillating at lower frequencies than body oscillators for the same stimulation and saturating at a lower threshold d_{high}.

Fig. 6B illustrates the dynamics of the above CPG model when the stimulation intensity d is varied. It can be clearly seen that there is a sharp transition between gaits at time 20 s by linearly increasing stimulation. During walking (i.e., at low stimulation levels $d_{low} < d < d_{high}^{limb}$), the strong couplings between limb and body oscillators cause the body's CPGs to exhibit low-frequency oscillations in the form of a standing wave. At $t = 20$ s when $d_{high}^{limb} < d < d_{high}^{body}$ there is a suppression of limb oscillator oscillations and a rapid transition of the gait into a higher frequency swimming mode. In doing so, the CPG of the body exhibits a running wave mode for

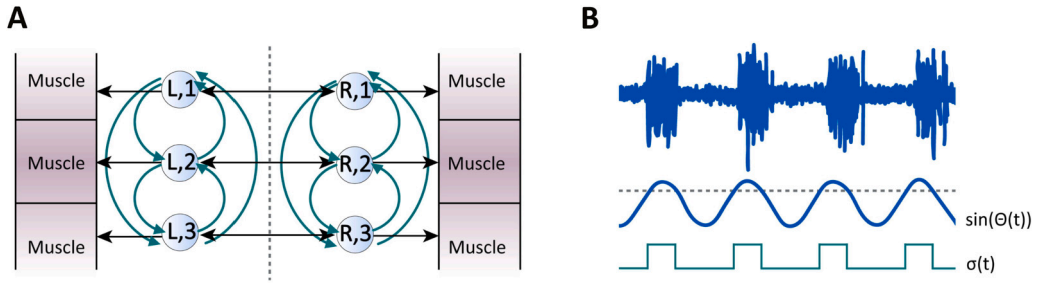

Fig. 7. (A) Configuration of the CPG model based on coupled phase oscillators with curvature feedback. Each oscillator is connected to every other oscillator on the same lateral ("Left" (L) and "Right" (R)) side (solid green lines). Within one segment the Left and Right oscillators are also coupled together and with muscles on the same lateral side (solid black lines). The curvature at each segment is calculated such that positive curvature curves in the direction of the right side measured from head to tail (oscillators are numbered from head to tail) (dotted gray lines). (B) Construction of a muscle activation wave from the CPG model. Source: adapted from [73].

swimming. These running waves increase in amplitude and frequency as the stimulation level is further increased, until the body oscillators stop oscillating at $d > d_{high}^{body}$.

3.2.4. *CPG model based on coupled oscillators with curvature feedback*

Another model of the CPG based on the coupled phase oscillators was proposed in the work [73]. This model was inspired to analyze a curvature feedback in the energetics and dynamics of lamprey swimming. To develop the lamprey CPG the authors used a pair of sinusoidaly coupled phase oscillators (one for the left lateral side and one for the right, see Fig. 7) to model the CPG segment:

$$\dot{\Theta}_{k,i} = \omega + \sum_{j=1}^{n} \alpha_{i,j} \sin(\Theta_{k,j} - \Theta_{k,i} - \psi_{ij}) + \alpha_c \sin(\Theta_{k,i} - \Theta_{k^*,i} + \pi) + \eta(k_i), \tag{6}$$

where $\Theta_{k,i}$ is the phase of the i-th oscillator, on the k-th side, where $k = 1$ correspond to the right side, and $k = 2$ correspond to the left side. The designation k^* determine the opposite. Side (in other words, if $k = 1$, then $k^* = 2$, and vice versa). The parameter $\omega = 2\pi$ is the natural frequency of these oscillators. The i-th oscillator on the k-th side is coupled to the other oscillators on the same side with strength given by

$$\alpha_{i,j} = \begin{cases} A_a \exp\left(-\dfrac{|i-j|}{\lambda_a}\right), & (i-j) < 0, \\ A_d \exp\left(-\dfrac{|i-j|}{\lambda_d}\right), & (i-j) > 0, \end{cases} \tag{7}$$

where $|i - j|$ is the number of segments between oscillator i and oscillator j, A_a, A_d, λ_d, and λ_a is the control parameters of coupling between oscillators. The asymmetry in the coupling strengths A_a and A_d is consistent with known experimental data [141,95]. The term $\alpha_c \sin(\theta_{k,i} - \theta_{k^*,i})$ in Eq. (6) represents the observed antiphase behavior between left and right segments which couples oscillator i on the k-th side to oscillator i on the opposite side. The term $\eta(k_i)$ captures proprioceptive feedback to the CPG system. Here k_i is the curvature of the lamprey midline at segment i, and the approach to choice of the functional form of feedback η can be found in Ref. [73].

Finally, the signal that the CPG sends to activate the muscle segment is modeled based on the phase of the oscillator on that side as shown in Fig. 7. Fig. 7B shows a typical bursting pattern from a typical CPG neuron in the lamprey [38] (top panel) and result of taking the sinusoidal signal of the phase of a model phase oscillator of the CPG (medium panel). Muscle is innervated when a signal from the CPG reaches a pre-defined threshold. Given a phase $\Theta(t)$, we define the time interval that corresponds to the segment being "active" to be those times when $\sin\Theta(t)$ is above a prescribed threshold γ. Fig. 7B, bottom panel, shows the procedure of extraction of an "on-off" activation signal $\sigma(t)$ from the phase $\Theta(t)$. For the phases along the segments on the lateral sides of the lamprey model (6), we have intervals of the muscle activation:

$$\sigma(t) = \begin{cases} 0, & \sin(\Theta) < \gamma, \\ 1, & \sin(\Theta) \geq \gamma. \end{cases} \tag{8}$$

In Ref. [175] we have already discussed in Section 3.2.2, it is assumed that local pressure sensation from lateral mechanoreceptor cells (such as the lamprey dorsal cells) forms local sensory-motor loops by proposing a simple feedback mechanism that is added to a CPG circuit. The feedback mechanism is determined by the relationship between animal body deformation and hydrodynamic forces during swimming movements. Thandiackal et al. shown that local body deformation and hydrodynamic forces are nearly in phase, with peaks of hydrodynamic forces arriving slightly before peaks of deformations. Motivated by this local phase locking, authors proposed a mechanism that entrains the swimming robot actuator activation that drives body deformation by constantly modifying its timing depending on the measured force signal. They implemented this mechanism in a coupled phase oscillator system represented by the following equations that describes the dynamics of the local activation x_i in a segmental circuit

$$\begin{aligned}\dot{\theta}_i &= \omega + \sum_j w_{ij}\sin(\theta_j - \theta_i - \phi_{ij}) + \epsilon \mathcal{F}_i z_i,\\ z_i &= \cos(\theta_i + \xi),\\ x_i &= \cos(\theta_i).\end{aligned} \tag{9}$$

The local activation signals x_i determine the muscle activity and hence the torque in the local joint of fish. The timing of $x_i(t)$ is controlled by the phase $\theta_i(t)$ of oscillators, whose time evolution is defined by intrinsic circle frequency ω (the same for all the segments); nearest-neighbor coupling weights w_{ij} ($w_{ij} \neq 0$ for $j = i-1$ and $j = i+1$), phase lag bias ϕ_{ij}, and the feedback mechanism based on the entrainment of the phase θ_i by the local hydrodynamic force $\mathcal{F}_i$ and a given feedback strength ϵ. $\mathcal{F}_i$ is the resultant normal force on a segment obtained from the difference of force readings from the left and right sensor plates. The feedback mechanism is defined by the sensitivity function z_i characterizing the response of the oscillator with phase θ_i to an external stimulus [85]. The phase delay ξ is determined by the way the stimulus perturbes the oscillator. In the animal, this phase delay is determined by the strength and sign (excitatory or inhibitory) of the synaptic connections from the dorsal cells to segmental circuits and by conduction delays. The model (9) is similar to the model (5) of Ijspeert et al. [84] of swimming CPG circuits already discussed above, but it differs from that work in the feedback mechanism.

All the models discussed above were characterised by the fact that they used nonlinear self-sustained oscillators as segments, which exhibit limit cycle behavior. However, Chen Wang et al. set out to design a much simpler CPG model for the locomotion control of the robot based on a system of coupled linear oscillators [188]. This design differs significantly from the usual CPG models in which nonlinear oscillators are commonly used. While other CPG keeps all the basic features of its biological counterparts and is capable of producing coordinated patterns of rhythmic activity, thanks to the linearity of the oscillators used, the computational costs of the CPG are greatly reduced and all the structural parameters can be selected easily. Wei Wang et al. showed the effectiveness of using a CPG model based on coupled linear systems to control the motion of an ostraciform fish robot [193]. This model allows generating different swimming modes and controlling the gait transition with only two input signals. CPG allows the robot to perform manoeuvrable swimming in three-dimensional space and automatically switch between thoracic and caudal gaits at different speeds.

3.3. Spiking neural network models

Following its biological counterpart, a CPG can be modeled by spiking neural networks that communicate through individual sequences of spikes. Instead of utilizing abstracted information signals, these networks employ pulse-coding mechanisms that enable the incorporation of spatial-temporal information. Theoretically, it has been demonstrated that these models are even more computationally powerful compared to those constructed with abstract neurons [115]. Furthermore, spiking neural networks (SNNs) offer promising solutions to problems in applied engineering while providing power-efficient capabilities, making them well-suited for applications in robotics [106]. However, CPG models based on spiking neural networks are relatively uncommon for implementation in robots compared to systems of coupled oscillators.

CPG models based on spiking neural networks are constructed using the Hodgkin-Huxley type of neuron models. Mathematically, the original Hodgkin-Huxley model consists of a set of nonlinear ordinary differential equations involving four variables: membrane voltage, activation and inactivation variables of the Na^+ current, and an activation variable of the K^+ current [77]. However, this model is computationally complex and expensive for simulating large populations of neurons. As a result, several simplified neuronal models such as the FitzHugh-Nagumo, Leaky Integrate-and-Fire model [167], and the Hindmarsh-Rose models have been used. These simplified models facilitate large-scale simulations of interconnected neurons that form a neural network. Most models based on neural networks investigate the problem of rhythmogenesis [148,178,103,111] and how rhythmic activity is generated by network properties, such as half-center networks [12,155]. They also explore how different oscillatory neural circuits become synchronized through interneuron connections [96,55], whether for intra-limb or inter-limb coordination.

A modeling study by Bicanski et al. (2013) [12] using spiking neural network approach demonstrated that a lamprey-like CPG network could potentially serve as a building block for axial and limb oscillators involved in swimming and stepping behaviors in salamanders. The study utilized a Hodgkin-Huxley type neuron model to describe the individual neurons. The CPG hemisegments consisted of sparsely connected populations of excitatory and inhibitory neurons, and were coupled to their contralateral counterparts. The model successfully replicated the experimentally observed effects of synaptic transmission blockade and modulation of ionic currents. Interestingly, the model demonstrated that modifications to neuronal conductance could control the frequency range of segmental oscillations. As a result, the lamprey-like CPG segmental circuit can be transformed into a salamander network, aligning with the idea of evolutionary conservatism in the locomotor systems from limbless vertebrates to tetrapods.

One of the early works that proposed an integrated approach combining the design of neuromorphic networks of spiking neurons with lamprey CPG models of motor control is the study by Donati et al. (2014) [50]. In their work, the CPG segment was modeled as a symmetrical network consisting of various groups of sparsely interconnected neurons, including motor neuron (MN), excitatory interneuron (EIN), lateral inhibitory neurons (LIN), and contralateral inhibitory neuron (CIN) (see Fig. 8). To capture the dynamics of a single neuron, the authors employed the classical adaptive-exponential integrate-and-fire (I&F) neuron model [13]:

$$C\frac{dV}{dt} = f(V) - w + I, \tag{10}$$

where the parameter C is the membrane capacitance, and I denotes the synaptic current. The function $f(V)$ describes the passive properties and the spiking mechanism and is defined as follows:

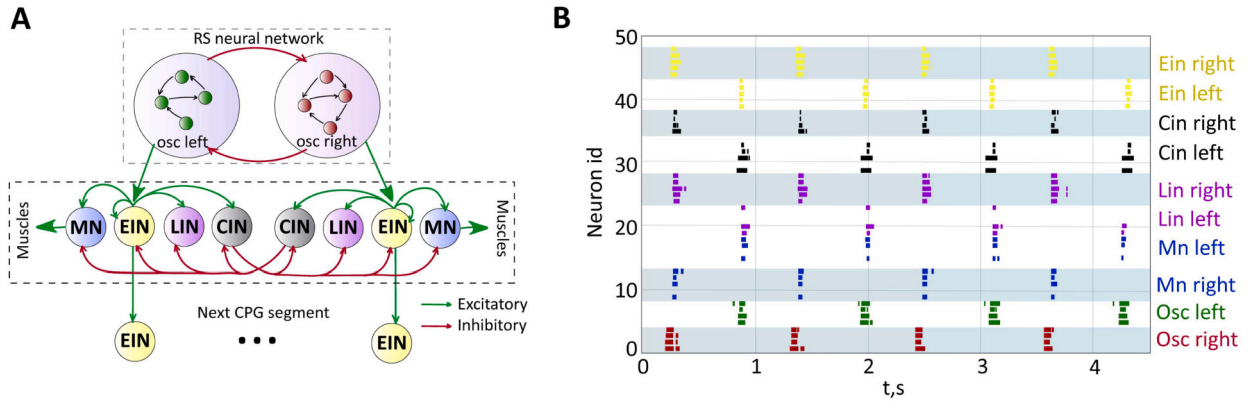

Fig. 8. (A) Configuration of the neuromorphic hardware lamprey CPG model [50]. The upper box represents an oscillatory network comprising two pools of neurons: osc left and osc right. The bottom box shows the CPG segment organisation, which includes the different types of neurons (EIN - Excitatory Interneuron, LIN - Lateral Inhibitory, CIN - Contralateral Inhibitory, and MN - Motor neurons. (B) Hardware model measurements. The oscillatory network produced spikes, alternating between the two populations: osc dx, osc sx. The right side of the segment is represented by a shaded background, while the left side is depicted with a white background. Source: adapted from [50].

$$f(V) = -g_L(V - E_L) + g_L\Delta_T exp\left(\frac{V - V_T}{\Delta_T}\right), \tag{11}$$

where g_L denotes the leak conductance, E_L is the resting potential, Δ_T represent the slope factor, and V_T is the threshold potential. w is the adaptation current, which can be represented by the following equation:

$$\tau_w \frac{dw}{dt} = a(V - E_L) - w, \tag{12}$$

where τ_w is a positive constant, and a denotes the level of subthreshold adaptation. The spiking CPG network model proposed in the study was implemented in real-time hardware using neuromorphic electronic circuits. This implementation allowed for direct control of the actuators in an artificial bio-inspired lamprey robot.

It has been demonstrated that a well-established CPG model [84], initially formulated as a system of coupled abstract oscillators, can be transformed into a spiking neural network that can be readily simulated using neuromorphic platforms [2]. The proposed spiking CPG neural network was successfully implemented on neuromorphic hardware and utilized to generate swimming gaits for a simulated lamprey robot model across various scenarios. Another study describes the design and implementation of a hardware-based neural network that emulates the oscillatory burst firing observed in the lamprey nervous system [128]. The authors introduce a novel hardware architecture capable of simulating the spiking behavior of lamprey neurons. Through their network, they successfully reproduce the coordinated oscillatory activity observed in the lamprey's CPG.

3.4. Biologically plausible and detailed CPG models

Due to the relative simplicity of the lamprey motor system as compared to mammals, it has been feasible to develop a comprehensive computational model based on experimentally derived facts ranging from the molecular-cellular level to that of networks and locomotion behavior. Simulations of this nature serve as an indispensable analytical tool, allowing us to assess the contributions of various components, such as different subtypes of ion channels [80]. This iterative process of modeling and biological experimentation enables researchers to investigate and refine their understanding of the system. Biophysically realistic models have been successfully developed for both the lamprey and the frog embryo systems.

In their seminal study [101], Kozlov and coauthors presented the first biophysically detailed, full-scale computational model of the lamprey locomotor CPG and its forebrain control. The simulated CPG consisted of 100 segments, each containing 100 neurons. The entire neural network was divided into two populations in a ratio of 60% excitatory and 40% inhibitory neurons. Each neuron was simulated using an spiking multi-compartmental biologically detailed lamprey spinal cell model [80]. Within each pool of model neurons, variability in neuronal size and membrane properties were experimentally proven. The architecture of synaptic connections between neurons in a segment and between segments was chosen based on experimental data. All 10,000 neurons were connected via 760,000 synapses, and the synaptic delay for each connection was estimated based on the distance between the neurons. In the model, the authors also presented the brainstem command system, as well as forebrain control from the basal ganglia with an additional 3,500 neurons. Supercomputer technologies were used for such large-scale simulations. These simulations showed that asymmetric anteroposterior synaptic connectivity in interneuronal populations, as well as variability in response properties within each neuronal population, play a crucial role in forming a constant phase lag along the spinal cord for different locomotor speeds. The study also revealed that the locomotor wave direction and steering can be flexibly controlled by local synaptic effects limited to only the very rostral part of the cord. To study visually guided lamprey locomotion, the reduced version of this CPG model was applied to a simulated animal swims around in a virtual environment containing visually detectable objects [89].

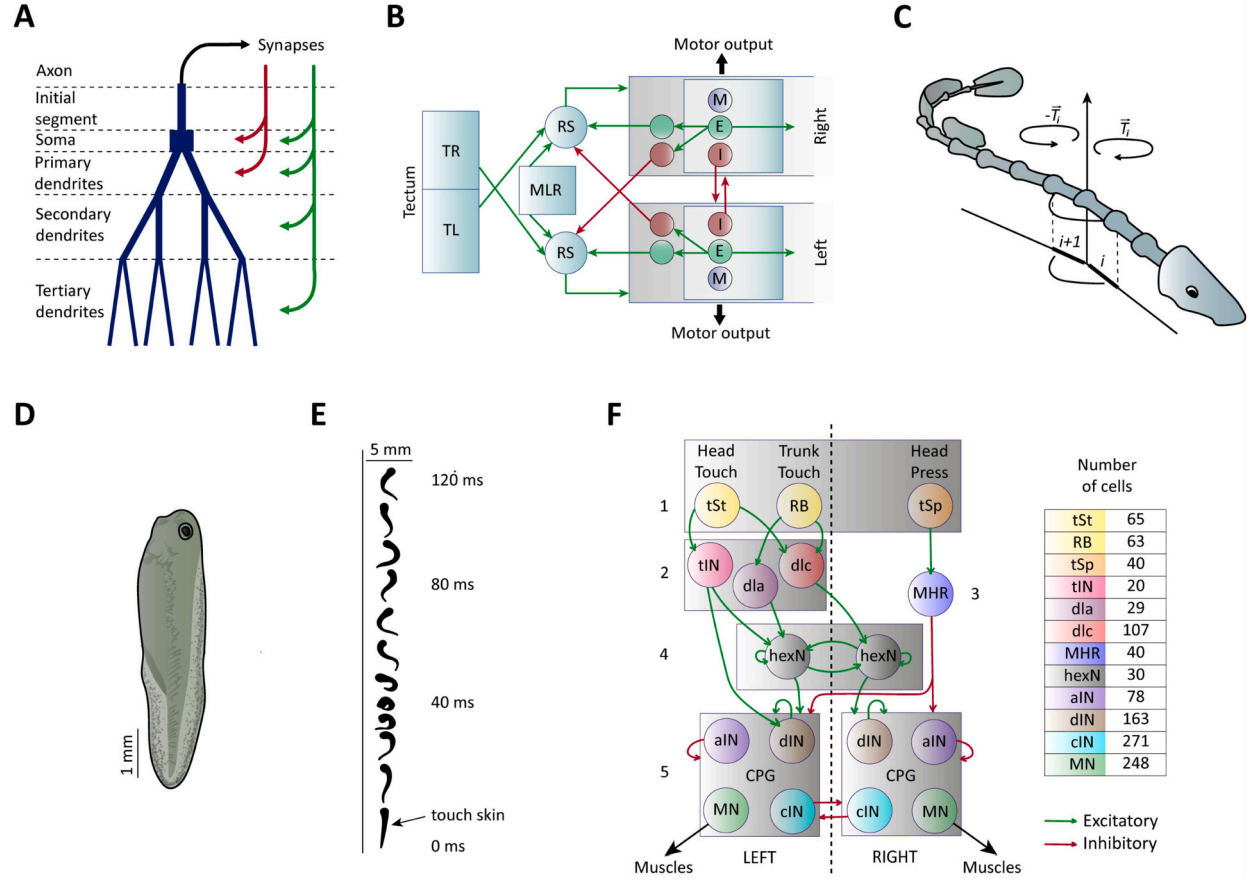

Fig. 9. Examples of a biologically realistic full-scale computational studies of CPG-based swimming. (A-C) Neuromechanical simulation of swimming in lamprey adapted from [102]. (A) The neuron model consists of 16 cylindrical compartments and includes multiple ionic channels. These channels are activated by synaptic inputs and are located on both the soma and dendrites of reticulospinal (RS) cells. Inhibitory synapses are depicted in red, excitatory synapses are represented in green. (B) The coordination of various neuronal populations is involved in the spinal and supraspinal locomotor networks. Tectal neurons (TL and TR), as well as symmetrically projecting neurons from the MLR, play a role in activating RS neurons on both sides. RS neurons provide excitatory input to the locomotor circuits in the spinal cord, depicted in gray. These circuits consist of a combination of excitatory cells (E), inhibitory cells (I), and motoneurons (M). The firing activity of the model motoneurons is integrated and directed towards 10 pairs of motor outputs. Additionally, information regarding locomotor activity in the rostral part of the spinal cord is fed back to the RS populations, represented by the large circles, through both excitatory and inhibitory afferent connections (indicated by green and red lines). (C) The lamprey body is modeled with 11 segments. The activation of a muscle at a specific joint, labeled as "*i*", is simulated by applying two opposing torques to the adjacent links. (D-F) Detailed modeling of frog tadpoles adapted from [58]. (D) Tadpole. (E) When touched (arrow), the tadpole first flexes to one side and then swims off. (F) The functional diagram depicts a CNS model network with 12 neuron types forming 5 layers.

In 2014, the authors used the detailed lamprey CPG model [101] as a basis to introduce a model of the brainstem-spinal cord network in lampreys [102] (Fig. 9A-C). A detailed control from higher brain centers is not required for the CPGs to generate the appropriate locomotor pattern. RS neurons in the brainstem activate CPG and these neurons also transfer commands from higher brain regions, such as turning signals from the optic tectum. It was shown experimentally that in both vertebrates and invertebrates, descending systems are phasically modulated via feedback from the CPG network during ongoing rhythmic movements. However, the physiological role of this modulation remained unclear. To explore this, Kozlov and co-authors used a biophysically detailed large-scale computational model of the lamprey brainstem-spinal cord network, which consisted of 19,600 multi-compartment spiking neurons and 646,800 synapses. The neuronal lamprey models can generate alternating activity patterns corresponding to forward and backward locomotion as well as steering to avoid obstacles. They discovered that the phase modulation of the reticulospinal activity from the CPG is crucial in generating steering/turning commands, and ensures reliable steering/turning commands without the need for precise timing of on- or offset. The simulations also predicted that steering/turning signals from the tectum can be gated by a CPG-related modulation of the reticulospinal neuron activity. This gating ensures that the steering commands are transmitted in the appropriate phase of a swimming cycle and suppressed out-of-phase. Finally, a biomechanical model of lamprey swimming was used to verify that the simulated neural network can control fish movements, including turning.

Another example of a biologically realistic full-scale computational study is recent modeling work that explored the role of the interplay between receiving sensory signals, decision making, and locomotion generation in a detailed model of the complete neuronal circuit of frog tadpoles [58] (Fig. 9D-F). The model includes the swimming CPG to generate rhythmic patterns, the brainstem, and sensory pathways upstream to make decisions. In particular, the model of the tadpole nervous system consists of approximately

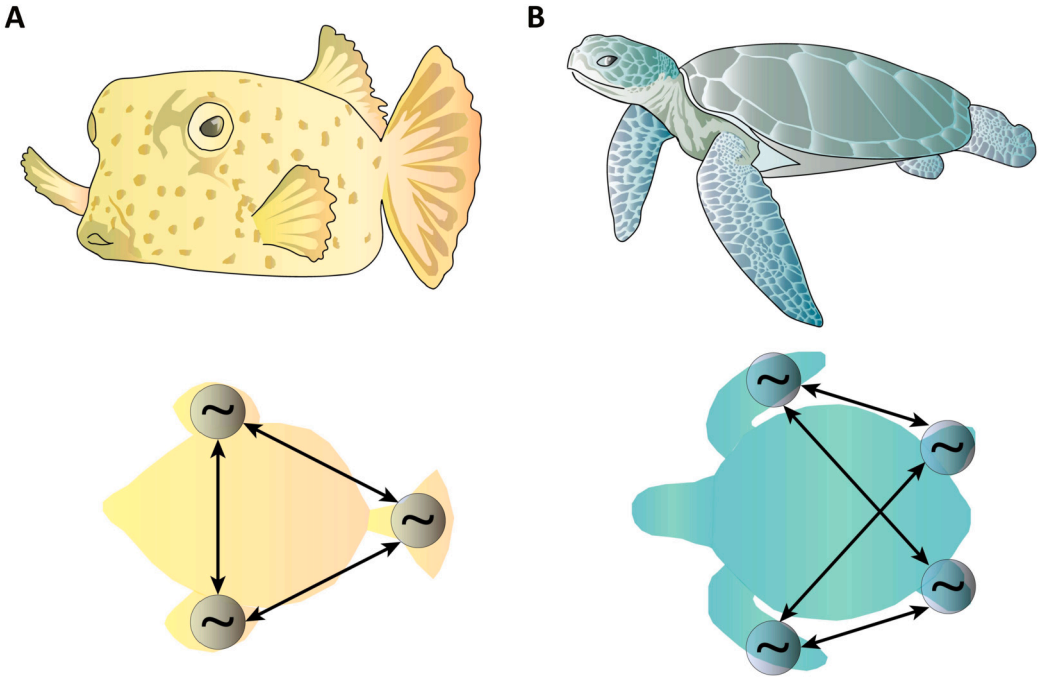

Fig. 10. (A) Boxfish's and (B) Turtle's CPG scheme. Sources: adapted from [43] (panels A) and [163] (panels B).

2300 neurons of 12 types of brain and spinal cord neurons that control swimming. To study tadpole responses to touch, the model includes two skin touch sensory pathways to initiate swimming, an inhibitory head skin pressure pathway to stop it, and hindbrain populations of sensory memory neurons that prolong signals from sensory pathways and activate RS neurons in the swimming CPG. Signals from the model were fed to a virtual tadpole biomechanical model of the whole-body musculoskeletal system to produce movements. Based on [137], the 3D virtual model reconstructs detailed anatomical and physical measurements of the shapes and mass distribution of the organs of real tadpoles. This model demonstrates realistic muscle innervation, body flexion, movement, body-water interaction, and, as the study results showed, provides reliable and realistic swimming.

3.5. CPG models with fins and limbs

Fish fins have evolved to serve several important functions. Let's dive into some key functions of fish fins:

1. Locomotion: Fish fins are primarily employed for swimming and maneuvering in the water. Different types of fins have distinct roles in movement. The dorsal fin aids in stabilizing the fish during swimming, while the caudal fin propels the fish forward.

2. Balance and stability: Fins also play a crucial role in helping fish maintain balance and stability in the water. The pectoral fins, situated on either side of the fish's body, act as stabilizers and enable the fish to make quick turns.

3. Temperature regulation: Certain fish, such as sharks, utilize their fins to regulate their body temperature. These fish possess specialized fins known as "gill slits", which allow them to pump water over their gills, effectively cooling their body temperature.

4. Communication: Fins can also serve as a means of communication for fish, enabling them to convey messages through specific fin movements or displays.

5. Protection: Some fish have developed specialized fins that provide protection against predators. For example, catfish have spines on their dorsal fin that can be deployed to deter predators from attacking.

When it comes to modeling central pattern generators (CPGs) with fins and limbs, there are a few different approaches. Fin segments can be incorporated as an addition to the dorsal CPG, or the model can exclusively consist of fin segments. Typically, models exclusively focused on fin segments are used to simulate the CPGs of boxfish, and less commonly, the CPGs of turtles.

For instance, in the article [43], the CPG chain consisted of three non-linear oscillators: two for the pectoral fins and one for the tail of the boxfish (Fig. 10A). The dynamics of the i-th oscillator were described by a system similar to equation (5).

In [194], the authors proposed the use of a nonlinear phase generator, which was initially introduced in [84] and [43], and linearized it using the first-order Taylor expansion to control the movement of each fin in the boxfish robot.

Yao et al. (2013) employed the same type of oscillator to construct the CPG chain for the turtle [203]. Each of the turtle's four flippers was assigned one oscillator.

In the paper by Seo et al. (2010), the authors also suggested implementing a CPG to govern a turtle robot [163]. The robot was maneuvered through the roll and pitch movements of its four flippers (Fig. 10B). The Hopf oscillator model was also utilized here. However, unlike the case described in Section 3.2, the oscillators do not form a chain to create the CPG. Instead, they function as a set of motor units: each flipper was associated with a single Hopf oscillator. The roll variable was denoted by x, and the pitch

variable was denoted by y. Since the turtle robot considered had 4 fins with 2 degrees of freedom per fin, the resulting dynamics were described by a system of 8 equations. It is interesting to observe how the movements of the fins enter a phase-locking state during walk, bound, and pronk modes in the CPG with a two-way ring architecture.

In salamander models, limb segments are employed for quadrupedal locomotion. During swimming, the limb segments are inactive due to their lower intrinsic frequencies compared to the swimming mode frequency (as well as the body CPG oscillators) [47]. The CPG segments of the limbs complement the CPG of the body. The additional intersegmental connectivity is usually organized in a manner that, when activated, the limbs force the body CPG circuit to produce standing waves, thereby implementing a walking gait with diagonally in-phase movements. To achieve this, the output connections should be stronger to suppress the tendency of the body CPG to produce traveling waves. The structure of the body CPG is inspired by the lamprey [84]. Another notable example is the study conducted by Liu et al. (2020), in which the authors proposed a spinal locomotor network model for salamanders. This model consists of interneuron networks, a motoneuron pool, and stretch reflex circuitry [113]. The outputs of the extensor (or flexor) interneurons are connected to the agonist motoneurons through excitatory synapses and to the antagonist motoneurons via inhibitory synapses.

4. Open-loop and closed-loop CPG models

A CPG generates rhythmic output patterns that can drive swimming behavior even in the absence of constant sensory input. This is possible because the CPG possesses intrinsic properties that enable it to generate oscillations and activity patterns without relying on external input. However, to initiate the rhythmic pattern of neural activity that governs fish locomotion, an initial stimulus or input is required to activate the CPG. Once activated, the CPG generates a coordinated pattern of muscle contractions that elicit swimming behavior, enabling the fish to move forward or backward at a constant speed.

For more complex fish movements, such as turning, obstacle avoidance, or chasing prey, the rhythmic pattern generated by the CPG needs to be adjusted online through input commands. This input can originate from various sources, including sensory feedback from the environment or other neural circuits involved in motor coordination.

When modeling CPG-based control systems for biologically inspired robots, evolutionary principles of feedback are often employed. Reactions to external stimuli can be categorized into two contrasting types: (i) almost instantaneous reflex reactions and (ii) decisions developed within neural circuits of the brain that involve conscious thought. The first case corresponds to low-level reflexes, which are involuntary and produce almost instantaneous movements in response to a stimulus. In the second case, the response is generated directly in the brain, with feedback signals and environmental information transmitted to an information fusion and control center.

Biomimetic robots have been developed that utilize the concept of the reflex arc and incorporate CPG models into low-level control systems [31,197,108]. Models of motor activity are also controlled by decision-making subsystems at higher levels. These subsystems incorporate information fusion mechanisms to process environmental information and other external signals [194,6,99]. Studies conducted on various robotic platforms to investigate adaptive movement in the environment using CPG and feedback (such as sensory receptors and sensory neurons) have led to defining the reflex as torque generation in the joint. In any case, the functioning of the control system emerges from an interaction between central commands and local reflexes [76], and field experiments have revealed that, for joints, reflexes take precedence over CPG outputs [97].

By activating these mechanisms, robotic fish can achieve swimming maneuverability and adaptability, allowing them to respond to changes in the external environment or proprioceptive information. In the fish brain, the mesencephalic locomotor region (MLR) governs the control of motor patterns (see Section 2.1 for details). Numerous studies have focused on understanding the mechanisms and circuits underlying the operation of the fish MLR, including its interaction with feedback loops.

The bioinspired model for integrating exteroceptive information and decision-making typically exhibits a complex structure. As a result, the control system can be hierarchical, involving multiple levels of sensory signal processing. For instance, in the case of robotic fish [99], data is acquired from at least three distance sensors and an inertial measurement unit (IMU) sensor. These sensory inputs are then filtered using the Environmental Data Processing Unit environmental data processing unit (EDPU). Subsequently, the decision mechanism-motion combination unit (DMCU) system generates an input that is fed to the CPG elements based on the current task. Feedback is sent to sensory neuron (SN), whose potentials are described by the equation (13) below. Finally, the result is transmitted to servos via motor neurons (MN).

$$\begin{cases} \tau_{res}\dot{x}_{(SN)i} = -x_{(SN)i} + p\lambda, & \lambda \geq \Lambda \\ \tau_{rec}\dot{x}_{(SN)i} = -x_{(SN)i}, & \lambda < \Lambda \end{cases} \tag{13}$$

Here, $x_{(SN)i}$ represents the membrane potential of sensory neuron (SN), τ_{res} and τ_{rec} denote the rise time constant and the fall time constant of the response generated in response to a stimulus, respectively. Moreover, p is the correction coefficient, λ represents the stimulus amount, and Λ denotes the threshold value.

In many existing studies, attempts have been made to modify open-loop models to incorporate feedback.

For instance, in the oscillatory CPG comprising a pair of coupled nonlinear oscillators [84], the original equation $x_i = r_i(1+\cos(\theta_i))$ has been replaced, as proposed by Manfredi et al. (2013), with the following equation [116]:

$$\varphi_i = r_i cos(\theta_i) + \Delta_i, \tag{14}$$

Here, φ_i represents the angle of the i-th joint. The additional term Δ_i allows the robot to modify its direction by introducing a deviation in the oscillation amplitude of its vertebrae. This deviation results in a curvature in the local region of the body, which propagates from the head to the tail. The modification of this control variable is determined by visual sensory inputs.

Another model presented in [207] is also based on Eq. (5) [84], mentioned in Section 3.2.3 above. However, the authors incorporated feedback obtained from liquid-level sensors into a single segment of the CPG. Consequently, the resulting model can be represented by the following system:

$$\begin{cases} \dot{\theta}_i = 2\pi\nu_i + \sum_j r_j w_{ij} sin(\theta_j - \theta_i - \phi_{ij}(u)), \\ \ddot{r}_i = a_i(\frac{a_i}{4}(R_i - r_i) - \dot{r}_i), \\ x_i = e_i + r_i cos(\theta_i)), \\ \ddot{e}_i = a_i(\frac{a_i}{4}(E_i - e_i) - \dot{e}_i), \\ \phi_{ij}(u) = \frac{\pi}{4}(\beta_i^j - \gamma_i^j sgn(u)). \end{cases} \tag{15}$$

Here, x_i represents the extracted output signal, which is adjusted by an oscillation offset e_i. The parameters β_i^j and γ_i^j correspond to factors associated with phase bias and the included sensory signal, respectively. The feedback signal associated with the i-th oscillator is denoted as u, and the sign function, $sgn(u)$, takes a positive value of "1" when the robot is on land and a negative value of "-1" when it is in water.

A slightly different approach to specifying feedback was applied in [73] using the CPG-based lamprey swimming model as an example (Fig. 11A-B). The scheme is based on utilizing proprioceptive signals from mechanoreceptors (edge cells) that sense stretch along the body. These signals, when stretch increases, excite the ipsilateral side and inhibit the contralateral side of the body. This type of deformation is tracked as a characteristic of body curvature, denoted as κ_i (where i is the segment number), and it appears in the main formula for the CPG phase generator (14) as a function $\eta(\kappa_i)$.

In this model, two forms of feedback were considered. The first is directional feedback, where oscillators are excited on one side and inhibited on the opposite side (or vice versa). The second is magnitude feedback, which provides a symmetric excitatory or inhibitory effect on oscillators on both sides. Both types of feedback influence the duration and frequency of body muscle activation. Magnitude feedback increases the frequency and swimming velocity, as observed in fish, but it decreases the amplitude, leading to slight differences. Directional feedback increases the duration of muscle activity, altering the degree of mutual activation between muscles on opposite sides of the body. This has more complex effects on swimming, such as changing the effective stiffness of joints [131]. In terms of swimming performance, there exists an optimal passive stiffness that guarantees the maximum swimming velocity [182].

4.1. Environmental feedback

Widely acknowledged findings suggest that while sensory feedback is not essential for generating rhythmic activity in CPGs, it plays a crucial role in adapting locomotion parameters to the environment. Sensory feedback must be included to close the control loop, ensuring mutual entrainment between the CPGs and the mechanical body, thereby enhancing animat or robotic locomotion [82,92,181]. The presence or absence of water is explicitly incorporated into the CPGs to modulate the coupling phase biases of the oscillators, thereby generating reactive behaviors.

However, despite the well-established hypothesis regarding the role of feedback in the generation of locomotor swimming patterns in lower fish and vertebrates, certain phenomena remain unexplained. For instance, there is evidence of the highest robustness of rhythm generation even in cases of complete spinal cord transection and a fictive motor activity regime at a reduced frequency [54,173,160]. Experimental studies involving the stimulation of lamprey dorsal cells have shown the activation of corresponding ipsilateral motor neurons and the inhibition of contralateral ones, indicating the presence of an additional circuit for rhythmogenesis [20]. Model studies have shown that hydromechanical feedback amplification below a spinal lesion can effectively restore lamprey swimming behavior, either partially or fully [72]. Furthermore, through a comprehensive research incorporating modeling, robotic experiments, and in silico study, the hydrodynamics of fluid flows at different fish stiffnesses were examined. This investigation aided in establishing the significance of environmental feedback, facilitated by a flexible body, in shaping the neuromechanical swimming pattern. Additionally, the study explored how this feedback influenced the resonant frequency and energy costs associated with swimming [183].

Robotic modeling that incorporates external hydrodynamic impact on a robotic lamprey equipped with mechanoreceptors has demonstrated that feedback can entrain CPG activity and contribute to rhythm coordination, ultimately increasing the frequency of swimming movements. This type of feedback can coordinate uncoupled neural oscillators to generate forward movement, enable the generation of rhythmic activity without the need for rhythmogenic neural oscillators, and provide redundancy, making exteroceptive and proprioceptive control circuits more robust against neural disruptions compared to either one alone [175] (Fig. 11C-D).

4.2. Command management

Studies involving robots that aim to mimic the behavior of fish and other underwater species often begin with preparatory stages of experimentation. During these stages, basic control schemes are employed for preliminary testing of swimming vehicles. One such control method involves using a joystick (manipulator), which allows for precise control of the robot's movements in the

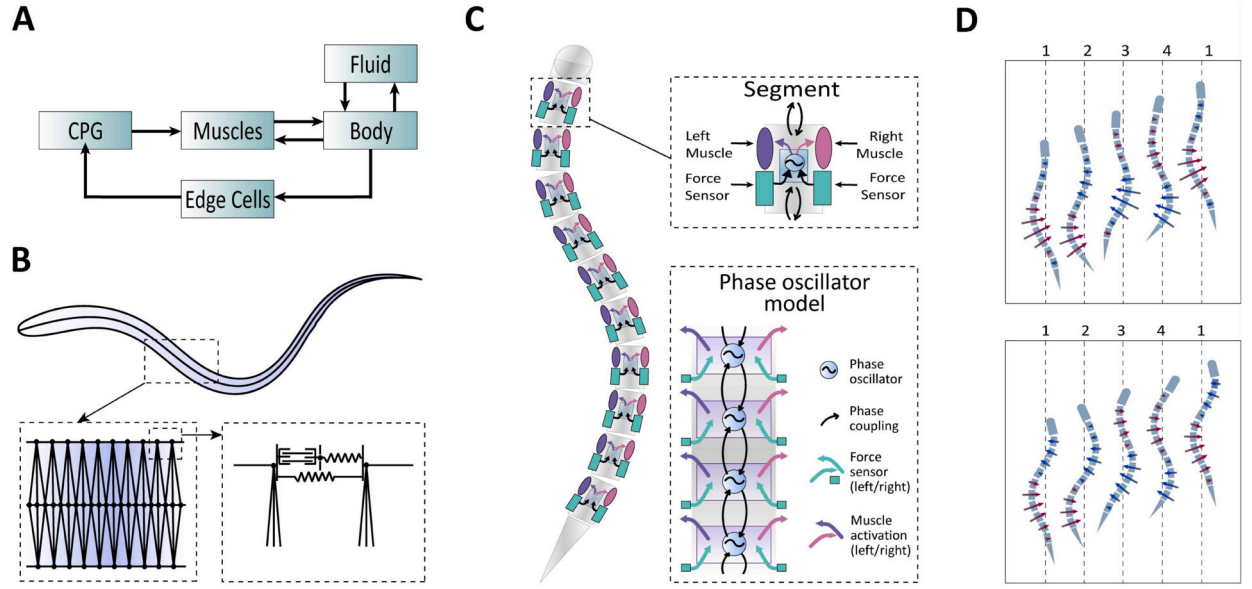

Fig. 11. (A) Schematic of feedback loop during locomotion. (B) The schematic depicts the body structure of a computational lamprey. The body consists of three filaments, with spring connections between discrete nodes within the filaments, generating passive elastic forces. Muscle segments connecting the nodes along the lateral sides contribute to force generation using a Hill-type model. Below the spring-mass damper system, there is an oscillator representing the skin of the lamprey. (C) The model consists of rigid body segments that are connected by actuated joints. Each segment has its own circuit, which includes oscillators and couplings. Additionally, each segment is equipped with left and right antagonistic muscles and a pair of lateral force sensors. (D) Examples of swimming with lateral forces on the left (red arrows) and on the right (blue arrows) during position control experiments. The top image shows modeling with a linearly increasing amplitude gradient from head to tail. The bottom image shows modeling with a constant amplitude along the body. Sources: adapted from [73] (panels A and B) and [175] (panels C and D).

underwater environment by a human operator when necessary [203]. For instance, this method may be used in conditions with low water transparency, presence of numerous dangerous obstacles (such as ice, algae, or man-made debris), or the need to comply with environmental standards and other safety precautions.

To develop swimming scenarios, real-time open-loop control schemes are implemented. An effective approach involves defining high-level macro-commands [201]. This method proves useful when specific targets need to be achieved, such as controlling the flapping frequency, cruising speed, or executing specific maneuver patterns.

4.3. Adaptive management

Despite the complexity involved in implementing an autonomous CPG-based control system with sensory feedback, a considerable number of researchers have successfully applied adaptive mechanisms to automatically adjust the swimming pattern. Adaptive control enables robots to navigate around static and moving obstacles [32,99,216], follow designated directions, and counteract hydrodynamic conditions in the underwater environment [32,185,202], as well as ensure smooth transitions between swimming gaits by adjusting the flapping frequency and amplitude [194,209].

When it comes to adaptive frequency tuning, the simplest versions of phase oscillators are often the most flexible. However, adaptive oscillators are also widely applicable in the design of CPG models. These range from Hopf and adaptive Rayleigh oscillators, to FitzHugh-Nagumo and adaptive Van der Pol oscillators. They are capable of synchronizing even with pseudo-periodic external stimuli, without compromising the generality of their dynamic learning approach [147].

5. CPG implementation in robotics

The development of fish robots is a complex process that involves various factors. Important aspects include electronics and software for autonomous operation, considering hydrodynamics to optimize body shape and fins for efficient movement, utilizing lightweight and durable materials, equipping sensors for control and environmental interaction, and employing special power sources for underwater operation. All these elements impact the swimming characteristics and efficiency of fish robots.

In this review, our exclusive focus is on advancements in developing locomotion CPGs and their applications in robotics. Summarizing the previous sections, CPG models offer distinct advantages as an alternative to methods like finite-state machines, sine-generators, heuristic control laws, and prerecorded reference trajectories [186,140]. Notably, CPG models demonstrate limit cycle behavior, generating stable rhythmic patterns that enable quick recovery from disturbances. They are particularly suited for modular robots [39,90,91,118], featuring multiple control parameters that facilitate locomotion modulation and the issuance of control signals by higher-level controllers and learning algorithms, replacing multidimensional motor commands. Moreover, CPG models ensure smooth trajectory generation, even in the face of sharp changes in control parameters, thus averting potential motor

damage due to sudden command changes [84,82]. By integrating sensory feedback signals, CPG models establish mutual interaction between the central pattern generator and the mechanical body [71,171,172,184].

Next, we will present the main achievements of recent years related to the use of locomotion CPGs in real robots and virtual animates. Sections 5.1 and 5.2 show the main goals and results of the research, and Tables 1 and 2 briefly describe the main characteristics of animates and robots implemented in the analyzed works, respectively. For convenience, in this section we have sorted the works by animals' type.

5.1. Animates (virtual robots) - biomechanical simulation

5.1.1. Lampreys

The studies focus on understanding how CPGs control locomotion in lampreys. They explore CPGs' neural dynamics, sensory feedback, and interactions within the brain-spinal cord system. These investigations aim to uncover the principles of neural locomotion control. Researchers intend to create computational CPG models and other neural networks for controlling movement, testing them with robotics. Their goal is to enhance robotic systems for navigation in complex environments. Objectives include developing CPG models for rhythmic and non-rhythmic motions, examining visual and curvature-based feedback, and designing energy-efficient spiking CPGs for neuromimetic hardware.

The following research explores bionic neural networks and CPGs for controlling fish-like robots and understanding visual behaviors in lampreys. Zhang et al. (2006) propose a bionic neural network with CPGs that effectively controls fish-robot motions [215]. Kamali-Sarvestani et al. (2013) investigate lamprey visual behaviors using a CPG-based neural network model, capable of executing appropriate reactions to different visual stimuli [89]. Kozlov et al. (2014) describe how the phasic modulation of reticulospinal activity in CPGs ensures reliable steering commands and validate their findings with a mechanical model of lamprey swimming [102]. Liu et al. (2018) propose a new locomotion control network capable of generating rhythmic and non-rhythmic movements, exhibiting simple mathematical structure and strong biological properties [111]. Overall, these studies highlight the effectiveness and adaptability of CPG-based control systems for underwater robots, showcasing their potential for real-world applications.

The next studies explore different aspects of CPG-based control systems, focusing on sensory feedback effects and the development of a new Spiking CPG model.

Hamlet et al. (2018) investigate the impact of body curvature-based sensory feedback on lamprey swimming performance [73]. Their simulations reveal that directional feedback modifies muscle activity duration while magnitude feedback increases beat frequency and reduces energetic cost. Such feedback with different forms creates distinct swimming performance outcomes. Angelidis et al. (2021) introduce a novel Spiking CPG based on high-level abstract coupled Hopf-like oscillators [2]. This flexible CPG model can be implemented on both software and neuromimetic hardware, allowing for a wide range of synchronized gaits and parameterizations. Their lamprey robot experiments validate the effectiveness of the CPG in regulating locomotion across various simulation scenarios. Furthermore, the researchers demonstrate the real-time operation of the controller, highlighting its potential advantages in terms of energy efficiency and computational speed. In summary, these studies deepen our understanding of sensory feedback effects on swimming performance and present a new Spiking CPG model with potential applications in robot locomotion control, showing promise for real-time operation and energy efficiency when implemented on neuromimetic hardware.

5.1.2. Salamanders

The studies [83,75] focus on understanding salamander locomotion, particularly the role of sensory feedback in gait generation and transition. They aim to identify neurons in spinal circuits that control different gaits, develop improved spinal locomotion models, and understand how limbs and body coordinate during locomotion. Researchers aim to uncover locomotion control principles, potentially benefiting the design of walking robots. For example, one study used simulations and found that specific CPG configurations were likely responsible for stable swimming and walking gaits resembling salamander locomotion [83]. Another study explored the importance of sensory feedback in gait generation, highlighting that proprioceptive inputs are crucial for walking coordination while trotting is influenced more by CPGs [75]. Gait transition from walking to trotting involves increased activity in the mesencephalic locomotor region and sensory inputs at the hip and scapula regions during the late stance phase.

The research articles [112,113,169] explore different aspects of salamander locomotion. One study introduces a novel neural network model to represent the spinal locomotor network, which can generate various gaits such as forward and backward walking, swimming, and turning, with smooth transitions controlled by external inputs from the brainstem [112]. Another study proposes an improved biomechanical model with modified forelimb structure and a new spinal locomotion network model. This enhanced model allows for generating different walking turning gaits, precise control of forelimb swing order, and rapid transient response speed [113]. Lastly, researchers develop a mathematical model based on CPG for understanding limb-body coordination during salamander locomotion. By incorporating limb-to-limb, limb-to-body, body-to-limb, and body-to-body feedback rules, the model replicates spontaneous gait changes and speed-dependent gait transitions observed in salamanders, highlighting the importance of sensory feedback in enabling flexible coordination [169].

5.2. Hardware implementation (electronic circuits, robots)

5.2.1. Anguilliform locomotion type (lampreys, eels)

Anguilliform locomotion involves undulating the entire body in a wave-like motion, used by aquatic animals like lampreys and eels for swimming. It is an efficient method for long-distance swimming, although not as fast as other forms of movement. Many

Table 1
Comparison of virtual animats by type and number of CPG segments, features of the sensory system and skills.

Animal	CPG Segment	Number of Segments	Feedback (Sensors)	Skills	Source
Lamprey	Nonlinear (Zhang) oscillator	18	One high level controller	Startup, stop, forward swimming, backward swimming and turn	[215]
Lamprey	Symmetric neural networks located on the left and right sides (100 IF neurons)	16	Tectum, MLR, RS neurons (retina)	The ability to distinguish objects of different colors: predators, obstacles and prey, respectively, and change behavior according to this information	[89]
Lamprey	Compartment models of 1960 neurons and 64680 synapses	10	Tectum, MLR, RS neurons	Forward swimming	[102]
Lamprey	2 inherent bursting neurons with mutual inhibition	40	-	Forward swimming, turn, non-rhythmic locomotion	[111]
Lamprey	Pair of sinusoidally coupled phase oscillators	320	Stretch mechanoreceptors (edge cells)	Forward swimming	[73]
Lamprey	Spiking network (280-2000 LIF neurons)	8	-	Forward swimming	[2]
Salamander	Nonlinear oscillator	16	Sensory stretch feedback only in the body segments	Swimming and walking	[83]
Salamander	25E and 15I compartment neurons [101]	40	MLR, stretch receptors	Swimming and walking	[75]
Salamander	[111] neurons	31 (24)	-	Forward and backward walking gait, swimming gait and turn	[112,113]
Salamander	Phase oscillator	15	Diagonality and waveform indices	Swimming and walking, gait transition from lateral sequence walking with standing body waves, to walking trot with traveling body waves	[169]

investigators and engineers are developing robots that mimic the movements of sea lampreys [196,116,222,205,175,33]. These robots use shape memory alloy actuators and an electronic nervous system (ENS) to control the undulating body. The ENS incorporates networks of map-based neurons and synapses, receiving input from exteroceptive sensors like compasses, accelerometers, inclinometers, and sonar arrays [196]. The CPGs in the ENS, based on physiological studies, coordinate the flexion waves for forward and backward swimming. The command network regulates reflexes, homing, orientation, and obstacle avoidance. Another article presents a biomimetic system inspired by the lamprey, featuring sensory receptors, muscle-like actuation, distributed control, and a vision system. The system showcases optimized swimming, goal-directed locomotion, high energy efficiency, and adaptive behavior [116] (Fig. 12A).

Researchers propose experiment-based approaches to improve biomimetic undulatory locomotion. One approach involves generating coordinated swimming gaits using artificial CPGs and optimizing the CPG model's parameters using a genetic algorithm (GA) to achieve optimal swimming speed and energy efficiency [222]. Additionally, a robotic lamprey design incorporating computer vision capabilities employs both frame-based and event-based cameras to stimulate the neural network, resulting in goal-oriented swimming. Event-based cameras enhance swimming trajectory accuracy and significantly improve visual input processing speed [205]. Another study investigates how hydrodynamic pressure forces can induce body movements in a robot mimicking neuromechanical systems. Self-organized swimming coordination is achieved through local feedback loops, providing resilience against neural disruptions and explaining post-spinal cord damage swimming abilities [175]. Moreover, a soft robotic eel with bidirectional bending segments controlled by a CPG exhibits flexible linear and turning motions, making it suitable for underwater exploration with limited space [33].

In summary, robots are designed for replication the undulating swimming motion of lampreys. On-line optimization and genetic algorithms enhance biomimetic locomotion. Computer vision capabilities and event-based cameras improve accuracy and speed in goal-oriented swimming. Hydrodynamic pressure forces and local feedback loops contribute to self-organized swimming coordination and resilience against neural disruptions. Meanwhile, soft robotic eels achieve versatile motions for underwater exploration. These advancements showcase the potential applications of biomimetic robotics in swimming and exploration tasks.

5.2.2. Ostraciiform locomotion type (boxfish)

Ostraciiform locomotion, observed in boxfish and trunkfish, involves using rapid oscillations of the tail fin for propulsion, creating vortices that aid in lift and reduce drag. Researchers have created fish robots, such as BoxyBot, that mimic this locomotion style, enabling swimming, crawling, and various movements using a CPG-based control system triggered by light, water, and touch sensors [105,43]. These robots exhibit agile behavior and generate stable rhythmic patterns despite changes in control parameters. Another study focuses on a robotic boxfish with a locomotion controller consisting of two layers – oscillators and a transition layer – to achieve flexible switching of swimming patterns and precise attitude control using sensory feedback from an IMU [193,194]. In addition, a bio-inspired robotic fish autonomously identifies and optimizes its swimming gait using a CPG, on-board sensor processing, and

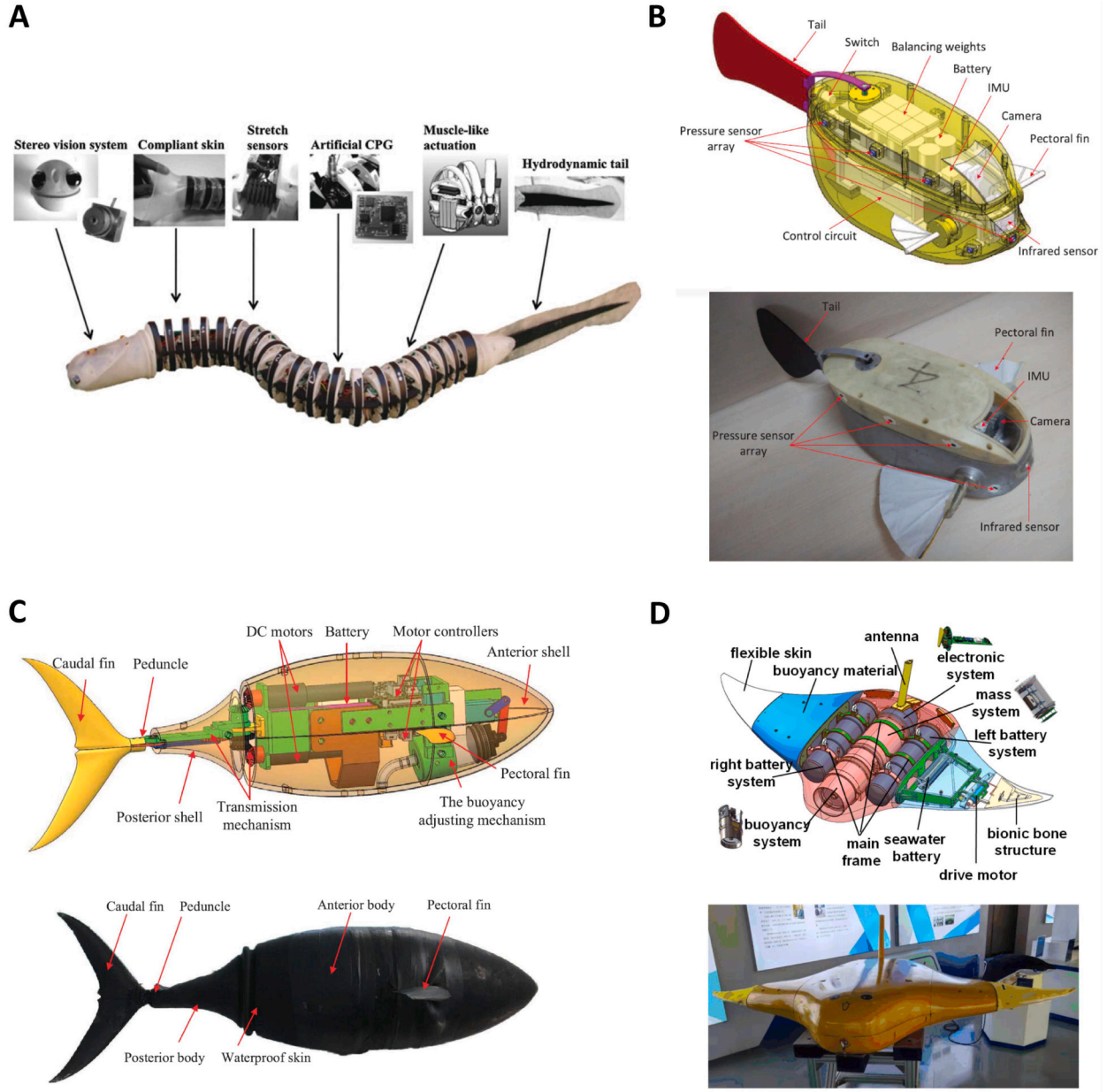

Fig. 12. Examples of implemented biomimetic robots. (A) Lamprey: anguilliform locomotion type [116]. (B) Boxfish: ostraciiform locomotion type [192]. (C) Tuna: thunniform locomotion type [51]. (D) Manta-Ray: rajiform locomotion type [214].

particle swarm optimization. The robotic fish achieves a maximum swimming speed of 1.011 BL/s (40.42 cm/s) through autonomous gait optimization [192] (Fig. 12B). The incorporation of CPG-based control, sensory feedback, and autonomous optimization algorithms contributes to the agility, precise control, and adaptive locomotion capabilities of these robotic fish. These studies pave the way for bio-inspired ostraciiform swimming robots with enhanced maneuverability and autonomy.

5.2.3. Subcarangiform locomotion type (pike)

The subcarangiform fish locomotion type involves strong body wave amplitudes, mostly in the rear half, leading to stiff hulls for speed but reduced maneuverability. In the work [219] authors designed a CPG model with nonlinear oscillators for a subcarangiform robotic fish, enabling coordinated swimming patterns and smooth gait shifts, while another study [109] presents a mathematically stable CPG model for microcontrollers, allowing online adjustments of physical outputs. Swimming patterns reproduced by a CPG model with connected neural oscillators can be diverse, that have been proven both theoretically and experimentally [211,191]. In [199], a flexible subcarangiform robotic fish uses CPG-based control for precise forward and backward maneuvers, with turning

variations. A self-propelled robotic fish with multiple control surfaces and vision system is explored in [210], achieving agility and speed through CPG control and visual feedback.

Many researchers focus on improving actuation, design, and control models. For instance, Wu et al. find small phase lags boost swimming [198], Yu et al. optimize control for faster swimming [213], Yang et al. ensure fault tolerance [202], Wang et al. optimize speed and efficiency [190], Xie et al. study body patterns' effects on cruising [200]. Overall, they refine fish-like locomotion, optimizing speed, efficiency, and control for practical use.

5.2.4. Carangiform locomotion type (shark, carp)

Carangiform locomotion is characterized by fast, stiff movements concentrated in the rear. The engineering studies focusing on controlling this type of robotic fish include designing: a neural-based control method for a modular fish steering [79]; a linear CPG control architecture, reducing computational cost and using only two control parameters for locomotion [188]; a centralized system to coordinate multiple fish using fuzzy reinforcement learning (RL) [209]; a CPG control system and sensor feedback, improving swimming ability of the robotic shark [206]; an autonomous carp-like fish prototype with biomimetic control [5]. Abovementioned works advance robotic fish control, achieving different swimming patterns, coordination, and biomimetic design.

Several studies contribute to the field of biomimetic robotics by advancing the control mechanisms and capabilities of robotic fish, including autonomous swimming, obstacle avoidance [32], rigorous control with efficient maneuvering [201], precise path-following [217], especially applying novel artificial intelligence (AI) techniques [6,99].

5.2.5. Thunniform locomotion type (tuna)

The thunniform type of fish, such as tunas and certain sharks, are fast and efficient swimmers with a distinctive body shape emphasizing tail and peduncle movement for increased speed and prey capture. Numerous studies in the field of biomimetic robotic fish draw inspiration from the thunniform group, translating their impressive swimming capabilities into innovative designs, for examples see [78,216,51]. In the first work Hu et al. replicate thunniform kinematics, achieving a maximum speed of 2.0 m/s in their biomimetic robotic fish using a four-bar propulsive mechanism and a CPG controller [78]. The second research by Zhang et al. combines insect wings and fish fins in their design, resulting in enhanced agility and stability [216]. Their robotic fish showcases versatile maneuvering and obstacle avoidance abilities enabled by a CPG model. Lastly, Du et al. focus on fast swimming and effective maneuvering, creating CasiTuna (Fig. 12C), a robotic fish with a unique two-motor-actuated propulsive mechanism [51]. The integration of CPG-based control, unique propulsion mechanisms, and stabilizing features contributes to achieving faster speeds, versatile maneuverability, and promising potential for exploration and survey missions in aquatic environments.

5.2.6. Rajiform locomotion type (ray, dactylopteridae)

Rajiform locomotion, observed in rays, involves wing-like pectoral fin flapping that enables agile maneuvering. Researchers have developed biomimetic robotic manta rays for marine applications: RoMan-II, utilizing a CPG model with nonlinear oscillators for fin manipulation, allowing swimming and turning control [221]; Robo-ray, mimicking a cownose ray's motion using oscillating pectoral and tail fins [27]; a bionic robot with manta ray-like pectoral fins, using phase oscillators and closed-loop control for rhythmic motion and continuous mobility [74]. Experimental study verified that the robotic vehicle inspired by manta rays, combining gliding and flapping propulsion using flexible pectoral fins and a buoyancy adjustment system, can exhibit maneuverable flapping and efficient gliding, showing potential for marine applications [214] (Fig. 12D). Cao et al. optimize control parameters of a manta ray robot, achieving improved similarity to real manta ray motion through a similarity evaluation rule and enhanced CPG-based motion control signals [28]. Furthermore, Zhang et al. introduce a biomimetic underwater vehicle based on dactylopteridae movement, demonstrating stability and maneuverability with symmetrical fins and a double-joint fishtail [218]. Control methods involve CPGs and fuzzy adaptive proportional-integral-derivative (PID) controller. Coordinated control with CPG and fuzzy algorithms ensures realistic motion, high mobility, and stability in complex underwater environments. Engineering studies advance biomimetic robotic manta rays and dactylopteridae-inspired vehicles, showcasing control strategies, motion replication, stability, and maneuverability in marine environments.

5.2.7. Dorsoventral locomotion type (dolphin)

Dolphins are adept swimmers, utilizing their tail flukes, dorsal fin, pectoral fins, and body movements for propulsion and maneuverability. A new dolphin robot, discussed in [212], mimics dolphin swimming motions using a CPG network. The robot achieves smooth trajectory tracking and tests confirm the effectiveness of its design and control methods. Another instance – a robotic dolphin inspired by killer whales, outlined in [110], is designed for water quality monitoring. It employs powerful posterior body and fluke for speed, separate pectoral fins and yawing dorsal fin for maneuvering, and various sensors for autonomous monitoring. Controlled by a CPG-based controller, the robotic dolphin demonstrates forward swimming, turning, diving, and surfacing capabilities, with successful experimental and field testing. Dolphin-inspired vehicles, leveraging CPG-based control, allow for smooth and stable trajectory tracking and demonstrate potential for applications in areas such as water quality monitoring.

5.2.8. Turtle

Sea turtles have adapted limbs for swimming, with flattened paddles for propulsion and steering. They retract their limbs into their shells to increase hydrodynamics. Streamlined bodies and hydrodynamic shells minimize resistance. Buoyancy is regulated by controlling lung air and body angle. Sea turtles' limb adaptations, hydrodynamic design, and buoyancy control serve as inspiration

for the development of underwater vehicles employing CPG-based control, allowing for efficient swimming, maneuvering, and real-time data transmission. For instance, Seo et al. discuss a control method based on turtles' flapping fins. CPG control system generates synchronized oscillation patterns for position-served flapping fin actuators. Stability analyses and experiments validate the proposed framework [163]. Yao et al. present a turtle-like underwater vehicle controlled by CPG-based architecture [203]. Four oscillation flippers enable swimming and attitude control through adjusting angles, flapping frequency, and amplitude. The vehicle's utility and stability are demonstrated through experiments, with real-time transfer of underwater video information.

5.2.9. Amphibious

There are various amphibious animals that live both in water and on land. Depending on their preferences and habitat, amphibians exhibit different forms and types of locomotion. Researchers and engineers develop amphibious robotic systems inspired by natural creatures, showcasing innovative locomotion strategies, versatility in water and on land, improved efficiency in swimming modes, and novel leg designs for adaptive locomotion. Crespi et al. develop amphibious snake-like robots (AmphiBot I and II) [40,41] inspired by elongate vertebrates. Controlled by a CPG, the robots showcase swimming and snake-like ground movement, optimizing parameters for efficient locomotion. The AmphiRobot [49,48] imitates underwater locomotion, utilizing a wheel-propeller fin mechanism for versatile movement in water and on land. It performs various modes, including swimming, turning, and pitching. Yu et al. improve a previous model, enabling fish-like lateral swimming and dolphin-like dorsoventral swimming, with the latter achieving a 10.3% increase in speed compared to carangiform swimming [207]. Zhong et al. introduce Amphibex-II [220], an amphibious hexapod robot, with variable stiffness legs combining the advantages of walking legs and swimming flippers. The legs' stiffness can be adjusted manually, and a CPG neural network enables smooth gait transitions. Field experiments demonstrate the advantages of the leg design and control system.

5.2.10. Salamander

The CPG modeling of salamanders is largely based on the anatomy of elongated lampreys, a primitive eel-like fish. Notably, segments corresponding to the limbs of salamanders (limb CPG) exist alongside the spinal cord-based segments (body CPG). Simulation tasks primarily utilize oscillatory models with a low degree of biological plausibility, such as abstract oscillators [98,204,168] and bursting neurons [112,113]. To capture more detailed dynamics, researchers have explored the use of more complex IF neurons [75,98]. Electrophysiological investigations have revealed the role of glutamatergic synapses in generating rhythmic bursts and inhibitory glycinergic neurons in coordinating alternating activity between the lateral sides of the salamander [158]. This has motivated the utilization of spiking neurons, a simplified version of the multicompartment Hodgkin-Huxley model employed by Wallen et al. [187].

The synaptic couplings within the network topology also play a crucial role in salamander CPG systems. Salamanders exhibit two frequency-dependent modes: lamprey-like swimming with undulatory waves at high oscillatory rates and trot gait, where the limbs walk in anti-phase with standing waves at low oscillatory rates. Thus, the internal and inter-segmental connectivity of body CPG and limb CPG neural circuits are essential for reproducing these movements. Significant contributions have been made by scientific groups such as Ijspeert et al. [84,75,98,12] and Liu et al. [111–113], who explored various topologies to embody these ideas.

6. Discussion & future perspectives

We have conducted a comprehensive review of modern studies dedicated to underwater swimmers, covering aspects ranging from basic features of animal physiology to the organization of movement and motor control. Additionally, we explored the design and development of mathematical models for CPGs, as well as simulations of virtual swimming robots and the design of real hardware. Based on our analysis of the current state-of-the-art in this field, we can outline the following key points for discussion: (i) What mechanisms of underwater movement control have not been adequately studied and need to be addressed in future fundamental studies? (ii) What aspects should be further refined and elaborated upon in mathematical models for the motor control of swimmers? (iii) What advancements in design and technologies are necessary to achieve true biomimetic swimming, considering factors such as kinematics, control, and energy efficiency?

By addressing these questions, we aim to advance the understanding and development of underwater swimmers, ultimately striving for more realistic and biomimetic swimming capabilities.

(i) It is evident that our understanding of the motor control mechanisms underlying swimming at the cellular and molecular levels is still far from complete. There is much to explore regarding the principles of signaling and plasticity, as well as the cross-talk between central and peripheral neuronal circuits. While the organization and signaling of CPG networks have been well-elaborated upon, various aspects of motor control still remain unclear [68]. As mentioned in the introduction, CPGs play a crucial role in the organization of movement for aquatic creatures. Consequently, the modeling of CPGs has stimulated technological developments in the design of fish robots capable of different types of locomotion [43,221,116,78,110,200]. One area that requires further investigation in motor control is the interplay between the central and peripheral nervous systems, including the integration of sensory information and the generation of corresponding motor commands. Another aspect is the "fine tuning" of non-principal fins, for example, which are controlled by a number of motor neurons but are not critical for locomotion. This brings us to the challenge of simultaneously adjusting a large number of parameters, whether independent or interconnected, to generate an "optimal" pattern of muscle contraction for a specific motor command. One possible approach to tackling this task is to consider an artificial intelligence (AI) perspective by designing specific artificial neural networks. In this case, training datasets that establish the correspondence between motor patterns and resulting movement modes need to be curated and designed. For example, in the past decade, numerous

Table 2
Comparison of robots by type and number of CPG segments, features of the sensory system, performance indicators and skills.

Animal (swimming type)	CPG Segment	Number of Segments	Sensors	Performance indicators	Skills	Source
Lamprey (anguilliform)	discrete time map (DTM) [154,165,153]	10	digital signal processor (DSP) chip (sonar DSP, compass and accelerometer)		Forward and backward swimming, speed control and turning, homing on a sonar beacon, climb and dive, distinguish collisions from impediment	[196]
Lamprey (anguilliform)	Nonlinear oscillator [84]	7	Extra- and proprioceptive sensory receptor (stretch sensors) and a stereo vision system (two 2D complementary metal oxide semiconductor (CMOS) cameras)	Max speed: U = 0.25 BL/s (BL/s – body length per second); run time = 5 h	Goal-directed locomotion (Visuo-coordination) at different speeds	[116]
Lamprey (anguilliform)	Hopf oscillator	4, 6, 8	Strain gauge-based force sensors	Max speed: U = 0.65 BL/s; energy-efficiency index: I_E = 0.23 BL/J	Swimming forward at different speeds	[222]
Lamprey (anguilliform)	Symmetric neural networks located on the left and right sides (100 IF neurons) [89]	16	Frame-Based Object Detection: pair of XIMEA MU 9 PCMH RGB cameras; Event-Based Object Detection: pair of iniVation mini-eDVS cameras	Gaze misalignment scores for the two types of camera: 1) frame-based cameras: $\overline{M}_{gaze}$ = 3.34° s; 2) event-based cameras: $\overline{M}_{gaze}$ = 0.57° s	Approach behavior (attacking prey) and escape behavior (fleeing predators)	[205]
Lamprey (anguilliform)	Matsuoka oscillator [123]	10	Head unit for computations, exteroceptive force sensors	Max speed: U = 0.4 m/s; run time = 0.5 h	Resilient to both communication failures between segments and to sensor failures	[175]
Eel (anguilliform)	Phase oscillator	3	-	Max speed: U = 0.2 m/s; max turning velocity: 35.52° s^{-1}	Linear and turning motions	[33]
Boxfish (ostraciiform)	Nonlinear oscillator [84]	3	2 light, 1 touch, and 1 water sensors, 1 two-axis accelerometer	Max speed: U = 0.37 m/s	Swimming forward and backward, turning, rolling, moving up or down, and crawling	[43,105]
Boxfish (ostraciiform)	Linearized [84] oscillator through the first-order Taylor expansion	3	Inertial Measurement Unit (triaxial accelerometer, a triaxial gyroscope and a triaxial electronic compass) and camera	Max speed: 1.05 BL/s; run time = 1.5 h	Swimming forwards / backwards, turning left / right, swimming upwards / downwards and rolling clock wise / counter clock wise	[193,194]
Boxfish (ostraciiform)	Linearized [84] oscillator	3	Camera, IMU, pressure sensor array and infrared sensor	Max speed: 1.011 BL/s (40.42 cm/s); run time = 5 h	Swimming forwards / backwards, turning, and pitching	[192]
Subcarangiform	Nonlinear oscillator	6 (4 body and 2 pectoral fins)	Pressure sensor, camera	Max speed: 1 BL/s (65 cm/s); max angular velocity: 1.5 rad/s	Forward swimming and turning maneuver	[219]
Subcarangiform	Linear oscillator [188]	3	-		Forward / backward swimming and turning in sinusoidal oscillation; turning swimming in sawtooth oscillation	[109]
Subcarangiform	Nonlinear oscillator [84]	6 (4 body and 2 pectoral fins)	3 infrared sensors; 1 pressure sensor	Max speed: ≈38 cm/s	Forward / backward swimming, turning, pitching and combined maneuvers	[211,191]
Subcarangiform	Modified Hopf oscillator	4	Gyroscope, pressure sensor	Max speed: 57 cm/s (forward swimming), 25 cm/s (backward swimming)	Forward / backward swimming and maneuvering	[199]

(*continued on next page*)

Table 2 (*continued*)

Animal (swimming type)	CPG Segment	Number of Segments	Sensors	Performance indicators	Skills	Source
Subcarangiform	Nonlinear oscillator [212]	7 (4 body, 1 pelvic and 2 pectoral fins)	CMOS camera	Max speed: 1.36 m/s; max angular speed: 1.78 rad/s	Forward / backward swimming, turning, sideward swimming (pelvic fin), diving/surfacing	[210]
Northern pike (subcarangiform)	Hopf oscillator	8 (4 body and 4 pectoral fins – 2 for each)	Gyroscope, depth sensor	Max speed: 0.48 m/s	Forward / backward swimming, turning, diving, surfacing, and three pectoral motions (pitching, heaving, and heaving-pitching)	[198]
Subcarangiform	Hopf oscillator	4	-	Max speed: 1.15 BL/s	Forward / backward swimming	[213]
Northern pike (subcarangiform)	Pair of Hopf oscillator [198]	4	Feedforward compensator, feedforward-feedback controller		Forward / backward swimming	[202]
Pike (subcarangiform)	Hopf oscillator	6 (4 body and 2 pectoral fins)	Depth sensor and gyroscope	Max speed: 0.5648 m/s	Forward / backward swimming, turning and pitching	[190]
Subcarangiform	Hopf oscillator [190]	1	IMU	Max speed: 0.84 BL/s	Cruising, turning and ascending / descending	[200]
Carangiform	Matsuoka oscillator [123]	4 (2 tail and 2 pectoral fins)	Dual axis accelerometer	Max speed: 32 cm/s (forward swimming), 16 cm/s (backward swimming)	Forward / backward swimming, sharp turning, turning in advancing, submerging and ascending	[79]
Carangiform	Linear oscillator	3	-	Max speed: 38.2 cm/s	Forward swimming and turning	[188]
Carangiform	Linear oscillator	3	Vision-based multi object tracking subsystem	Max speed: 38.2 cm/s	2vs2 water polo game	[209]
Shark (carangiform)	Modified Hopf oscillator [199]	2	Infrared sensor, pressure sensor, light sensor, gyroscope	Max speed: 50 cm/s; run time = 1 h	Forward / backward swimming, turning, down and up, obstacle avoidance	[206]
Carp (carangiform)	Neural oscillator: two symmetric parts contains CIN, LIN, EIN and MN	2	10-DoF IMU, 3 infrared distance sensors	Max speed: 0.8516 BL/s; run time = 0.5 h; (Max speed: 1.36 BL/s; turning rate: 0.89 rad/s)	Forward, turning, up-down and autonomous swimming motions	[5] ([6,99])
Carp (carangiform)	[84] oscillator	1	IMU	Max speed: 1.37 BL/s; largest turning rate: 457°/s	Cruising, turning, stopping and transition among them	[201]
Black carp (carangiform)	[84] oscillator	1	IMU, 3 infrared sensors, pressure sensor	Angular error of direction tracking: less than 2°; run time = 2 h	Moving obstacle avoidance, direction tracking	[32]
Koi Carp (carangiform)	Linear oscillator [188]	3	Overhead camera	Max error: 0.212 m	Learning ability to move along the desired curve	[217]
Tuna (thunniform)	Hopf oscillator	2	Depth sensor, voltage sensor, current sensor and attitude heading reference system (AHRS)	Max speed: 2 m/s (1.69 BL/s); max turning rate: 58°/s; run time = 3 h	Forward swimming and turning	[78]
Two-tailed fish (thunniform)	Linear oscillator	6 (2 caudal fins and 4 pectoral fins – 2 for each)	Infrared sensors	Max speed: 1.21 BL/s	Avoid obstacles and realize autonomous swimming	[216]
Tuna (thunniform)	Hopf oscillator-based	2	-	Max speed: 0.8 m/s (1.52 BL/s); max turning rate: 80°/s	Straight swimming and maneuverability: yawing, pitching and turning	[51]
Manta ray (rajiform)	Hopf oscillator	6 (3 for each 2 pectoral fins)	Water pressure sensor	Max speed: 0.4 m/s (0.8 BL/s); run time = 6 h	Swimming by flapping fins and turning	[221]

Table 2 (*continued*)

Animal (swimming type)	CPG Segment	Number of Segments	Sensors	Performance indicators	Skills	Source
Cownose ray (rajiform)	Phase oscillator	8 (3 for each 2 pectoral fins, 2 tail)	Gyroscope and depth gauge	Max speed: ≈0.66 BL/s (≈0.38 m/s); depth error: less ±100 mm; course error: less ±3°; run time = 2 h	Forward swimming, turning, sinking and rising	[27]
Cownose ray (rajiform)	Modified [84] oscillator	8 (3 for each 2 pectoral fins, 2 tail)	Pressure sensor, epth sensor	Max yaw angle rate: 62°/s	Forward swimming and turning	[74]
Manta ray (rajiform)	Modified [84] oscillator	7 (3 for each 2 pectoral fins, 1 tail)	Attitude sensor	Similarity value of the overall motion pose (with real fish): 88.53%	Forward swimming and turning	[28]
Manta ray (rajiform)	Modified [84] oscillator	4 (2 for each 2 pectoral fins)	Distance sensor, attitude sensor, ranging sensor	Max load: 20 kg	Swimming and gliding, adapts to harsh underwater environment	[214]
Dactylop-teridae (rajiform)	Hopf oscillator [213]	8 (3 for each 2 pectoral fins, 2 tail)	Pressure sensor, AHRS, water quality sensor	Max speed: 0.86 BL/s; min turning radius: 0; run time = 3 h	Forward swimming, diving/floating motion, turning maneuver, fixed depth hovering, and directional cruise	[218]
Dolphin (dorsoventral)	Hopf oscillator	5 (Moving Slider, Turning Unit, 2 Multijoint Tail, Fluke)	Pressure Sensor, infrared detector	Max speed: ≈1.1 BL/s; min turning radius: ≈0.4 BL; run time = ≈2 h	Forward / backward swimming, turning underwater, pitching, and heaving	[212]
Dolphin (dorsoventral)	Hopf oscillator [213]	5 (2 flippers, dorsal fin, waist and caudal joints)	Inertial navigation system, global positioning system (GPS), depth sensor, infrared sensors	Max speed: 0.42 m/s; run time ≈3 h	Forward Swimming, turning, diving and ascending, water quality monitoring	[110]
Turtle	Hopf oscillator	4 (1 for each limb)	Direct sensory feedback from servos to CPG		Pronk, walk, and bound gaits	[163]
Turtle	[84] oscillator	4 (1 for each limb)	GPS, gyroscope, accelerometer, depth transducer and magnetometer		Forward / backward swimming, Yaw, ascending, submerging, rotation	[203]
Snake (anguilliform)	Nonlinear oscillator	8	-	Max speed: 0.035 m/s	Swimming and crawling	[40]
Snake (anguilliform)	Nonlinear [84] oscillator	8	-	Max speed: 0.4 m/s – crawling; 0.23 m/s – swimming	Swimming and crawling	[41]
Amphibious (carangiform)	Nonlinear [84] oscillator	10 (2 for pectoral fins, 6 for body, 2 for caudal fins)	3 infrared sensors, 1 pressure sensor, 2 liquid-level sensors	Max speed: 0.38 m/s; run time ≈1 h	Forward / backward locomotion in water and on land, turning and pitching	[49,48]
Amphibious (carangiform and dorsoventral)	Nonlinear [84] oscillator	12 (2 for each 2 pectoral fins, 6 for body, 2 for caudal fins)	infrared sensors, pressure sensor, liquid-level sensors	Max speed: 1.16 m/s; run time ≈2 h	Forward / backward locomotion in water and on land, turning and pitching, dolphin-like dorsoventral and fish-like lateral swimming	[207]
Hexapod amphibious	Hopf oscillator	6 (1 for each 6 legs)	-	Max speed: 0.36 m/s – on land; 0.18 m/s – underwater	Swimming and walking	[220]
Salamander	Nonlinear oscillator	20 (1 for each 4 legs, 16 for body)	-		Swimming and walking	[84,42]

works have been published on the application of reinforcement learning (RL) approaches for controlling bioinspired robots. This method, when implemented on artificial neural networks, is well-known for surpassing the performance of most AI-based learning algorithms and achieving human-comparable levels [127]. RL's major advantage lies in its broad applicability, even when the system equations are unknown, nonlinear, non-differentiable, or only partial states are observable. However, it is important to note that recent studies have highlighted the less reliable outcomes of RL-based training, which necessitates extensive time, training data, and insight into relevant hyperparameters [152]. Nevertheless, successful methodologies have been developed to build control systems based on CPGs for various robot types. The evolution of these models can be traced through works exploring the dynamics of bipedal robots incorporating CPG with recurrent neural networks [129], quadripedal robots utilizing phase oscillator-based CPG [189], and soft snake robot governed by Matsuoka oscillatory CPG network [114], which exhibit movement patterns highly correlated with

those of lampreys. The field of swimming robotic fish also features robotic solutions. Recent references, such as [209,217,177], discuss the use of oscillatory CPGs for fish-like robots, and a noteworthy review by Tong et al. (2023) [176] provides valuable insights. Importantly, the training results of the employed neural networks align with the parameters in the models.

(ii) In the realm of mathematical modeling, in addition to the aforementioned AI networks for fine-tuning, there is still a lack of detailed biophysical models for control circuits that can be both biologically accurate and mathematically robust. Such models are needed to accurately simulate neuronal circuits and imitate pattern generation in CPGs [64]. On the other hand, simplified CPG networks composed of nonlinear oscillators exhibit auto-oscillations and multistability. However, due to their limited number of control parameters, it is challenging to integrate them with highly diverse and multi-parameter sensory networks and the "fine-tuning" system.

(iii) In general, there is now a fundamental understanding of locomotion control in CPG, and well-developed mathematically elaborated oscillatory models for CPGs. These advancements provide a solid foundation for designing a new generation of underwater fish robots capable of closely imitating basic types of aquatic movement [190,205,99,32,51,218]. From a technical standpoint, these robots operate with low-dimensional control systems that are well-integrated with state-of-the-art actuators, primarily servomotors. However, due to their size and relatively high energy consumption, it is challenging to incorporate a large number of such actuators into the robot's frame. This presents a technological limit in biomimetic design, in addition to the theoretical "fine-tuning" issue mentioned earlier. A potential technological breakthrough in this field that could enable true biomimetic robots lies in the development of artificial muscles based on new smart materials.

Declaration of competing interest

The authors declare that they have no known competing financial interests or personal relationships that could have appeared to influence the work reported in this paper.

Acknowledgements

The reported study was funded in part by the federal academic leadership program "Priority 2030" of the Ministry of Science and Higher Education of the Russian Federation (Sections 1-4) and in part by Russian Science Foundation Grant No. 21-12-00246 (Section 5). AEH thanks the grant SPbU (ID 94034465) (Sections 3.1 and 3.2).

References

[1] Manira AEl, Pombal MASG. Diencephalic projection to reticulospinal neurons involved in the initiation of locomotion in adult lampreys lampetra fluviatilis. J Comp Neurol 1997;389:603–16.
[2] Angelidis E, Buchholz E, Arreguit J, Rougé A, Stewart T, von Arnim A, et al. A spiking central pattern generator for the control of a simulated lamprey robot running on SpiNNaker and loihi neuromorphic boards. Neuromorphol Comp Eng 2021;1:014005. https://doi.org/10.1088/2634-4386/ac1b76.
[3] Arber S. Organization and function of neuronal circuits controlling movement. EMBO Mol Med 2017;9:281–4. https://doi.org/10.15252/emmm.201607226.
[4] Armstrong DM. The supraspinal control of mammalian locomotion. J Physiol 1988;405:1–37. https://doi.org/10.1113/jphysiol.1988.sp017319.
[5] Ay M, Korkmaz D, Koca GO, Bal C, Akpolat Z, Bingol M. Mechatronic design and manufacturing of the intelligent robotic fish for bio-inspired swimming modes. Electrom 2018;7:118. https://doi.org/10.3390/electronics7070118.
[6] Bal C, Ozmen Koca G, Korkmaz D, Akpolat ZH, Ay M. CPG-based autonomous swimming control for multi-tasks of a biomimetic robotic fish. Ocean Eng 2019;189:106334. https://doi.org/10.1016/J.OCEANENG.2019.106334.
[7] Batueva I, Tsvetkov E, Sagatelyan A, Buchanan J, Vesselkin N, Adanina V, et al. Physiological and morphological correlates of presynaptic inhibition in primary afferents of the lamprey spinal cord. Neuroscience 1999;88:975–87. https://doi.org/10.1016/s0306-4522(98)00239-5.
[8] Bear M, Connors BPMA. Neuroscience: exploring the brain. enhanced edition. Internationale Aufl; 2016.
[9] Bem T, Cabelguen JM, Ekeberg, Grillner S. From swimming to walking: a single basic network for two different behaviors. Biol Cybern 2003;88:79–90. https://doi.org/10.1007/s00422-002-0340-3.
[10] Berg EM, Mrowka L, Bertuzzi M, Madrid D, Picton LD, Manira AE. Brainstem circuits encoding start, speed, and duration of swimming in adult zebrafish. Neuron 2023;111:372–3864.e. https://doi.org/10.1016/j.neuron.2022.10.034.
[11] Bernau NA, Puzdrowki RL, Leonard RB. Identification of the midbrain locomotor region and its relation to descending locomotor pathways in the atlantic stingray, dasyatis sabina. Brain Res 1991;557:83–94. https://doi.org/10.1016/0006-8993(91)90119-g.
[12] Bicanski A, Ryczko D, Knuesel J, Harischandra N, Charrier V, Ekeberg Ö, et al. Decoding the mechanisms of gait generation in salamanders by combining neurobiology, modeling and robotics. Biol Cybern 2013;107:545–64. https://doi.org/10.1007/S00422-012-0543-1.
[13] Brette R, Gerstner W. Adaptive exponential integrate-and-fire model as an effective description of neuronal activity. J Neurophysiol 2005;94:3637–42. https://doi.org/10.1152/jn.00686.2005.
[14] Brocard F, Dubuc R. Differential contribution of reticulospinal cells to the control of locomotion induced by the mesencephalic locomotor region. J Neurophysiol 2003;90:1714–27. https://doi.org/10.1152/jn.00202.2003.
[15] Brown TG. On the nature of the fundamental activity of the nervous centres together with an analysis of the conditioning of rhythmic activity in progression, and a theory of the evolution of function in the nervous system. J Physiol 1914;48:18–46. https://doi.org/10.1113/jphysiol.1914.sp001646.
[16] Brownstone RM, Chopek JW. Reticulospinal systems for tuning motor commands. Front Neural Circuits 2018;12. https://doi.org/10.3389/fncir.2018.00030.
[17] Buchanan JT. Identification of interneurons with contralateral, caudal axons in the lamprey spinal cord: synaptic interactions and morphology. J Neurophysiol 1982;47:961–75. https://doi.org/10.1152/jn.1982.47.5.961.
[18] Buchanan JT. Commissural interneurons in rhythm generation and intersegmental coupling in the lamprey spinal cord. J Neurophysiol 1999;81:2037–45. https://doi.org/10.1152/jn.1999.81.5.2037.
[19] Buchanan JT. Contributions of identifiable neurons and neuron classes to lamprey vertebrate neurobiology. Prog Neurobiol 2001;63:441–66. https://doi.org/10.1016/s0301-0082(00)00050-2.
[20] Buchanan JT, Cohen AH. Activities of identified interneurons, motoneurons, and muscle fibers during fictive swimming in the lamprey and effects of reticulospinal and dorsal cell stimulation. J Neurophysiol 1982;47:948–60. https://doi.org/10.1152/jn.1982.47.5.948.

[21] Buchanan JT, Grillner S. Newly identified 'glutamate interneurons' and their role in locomotion in the lamprey spinal cord. Science 1987;236:312–4. https://doi.org/10.1126/science.3563512.
[22] Buchanan JT, Grillner S. A new class of small inhibitory interneurones in the lamprey spinal cord. Brain Res 1988;438:404–7. https://doi.org/10.1016/0006-8993(88)91373-x.
[23] Buchanan JT, Kasicki S. Activities of spinal neurons during brain stem-dependent fictive swimming in lamprey. J Neurophysiol 1995;73:80–7. https://doi.org/10.1152/jn.1995.73.1.80.
[24] Bullock TH, Hofmann MH, Nahm FK, New JG, Prechtl JC. Event-related potentials in the retina and optic tectum of fish. J Neurophysiol 1990;64:903–14. https://doi.org/10.1152/jn.1990.64.3.903.
[25] Cabelguen JM, Bourcier-Lucas C, Dubuc R. Bimodal locomotion elicited by electrical stimulation of the midbrain in the salamander notophthalmus viridescens. J Neurosci 2003;23:2434–9. https://doi.org/10.1523/JNEUROSCI.23-06-02434.2003.
[26] Caggiano V, Leiras R, Goñi-Erro H, Masini D, Bellardita C, Bouvier J, et al. Midbrain circuits that set locomotor speed and gait selection. Nature 2018;553:455–60. https://doi.org/10.1038/nature25448.
[27] Cao Y, Lu Y, Cai Y, Bi S, Pan G. CPG-fuzzy-based control of a cownose-ray-like fish robot. Ind Robot 2019;46:779–91. https://doi.org/10.1108/ir-02-2019-0029.
[28] Cao Y, Ma S, Cao Y, Pan G, Huang Q, Cao Y. Similarity evaluation rule and motion posture optimization for a manta ray robot. J Mar Sci Eng 2022;10:908. https://doi.org/10.3390/jmse10070908.
[29] Carbo-Tano M, Lapoix M, Jia X, Auclair F, Dubuc R, Wyart C. Functional coupling of the mesencephalic locomotor region and v2a reticulospinal neurons driving forward locomotion. bioRxiv, URL. https://doi.org/10.1101/2022.04.01.486703, 2022.
[30] Carrington AC, Secombes CJ. A review of CpGs and their relevance to aquaculture. Vet Immunol Immunopathol 2006;112:87–101. https://doi.org/10.1016/j.vetimm.2006.03.015.
[31] Chatterjee R, Matsuno F. Use of single side reflex for autonomous navigation of mobile robots in unknown environments. Robot Auton Syst 2001;35:77–96. https://doi.org/10.1016/s0921-8890(00)00124-x.
[32] Chen J, Yin B, Wang C, Xie F, Du R, Zhong Y. Bioinspired closed-loop CPG-based control of a robot fish for obstacle avoidance and direction tracking. J Bionics Eng 2021;18:171–83. https://doi.org/10.1007/s42235-021-0008-0.
[33] Chen Y, Wang T, Wu C, Wang X. Design, control, and experiments of a fluidic soft robotic eel. Smart Mater Struct 2021;30:065001. https://doi.org/10.1088/1361-665x/abf5ef.
[34] Christenson J, Boman A, Lagerbäck PÅ, Grillner S. The dorsal cell, one class of primary sensory neuron in the lamprey spinal cord. I. Touch, pressure but no nociception — a physiological study. Brain Res 1988;440:1–8. https://doi.org/10.1016/0006-8993(88)91152-3.
[35] Christenson J, Hill RH, Fulvia B, Sten G. Presence of low voltage activated calcium channels distinguishes touch from pressure sensory neurons in the lamprey spinal cord. Brain Res 1993;608:58–66. https://doi.org/10.1016/0006-8993(93)90774-h.
[36] Clarke JD, Hayes BP, Hunt SP, Roberts A. Sensory physiology, anatomy and immunohistochemistry of rohon-beard neurones in embryos of xenopus laevis. J Physiol 1984;348:511–25. https://doi.org/10.1113/jphysiol.1984.sp015122.
[37] Cohen AH. Control principles for locomotion-looking toward biology. Adaptive motion of animals and machines; 2006. p. 41–51.
[38] Cohen AH, Holmes PJ, Rand RH. The nature of the coupling between segmental oscillators of the lamprey spinal generator for locomotion: a mathematical model. J Math Biol 1982;13:345–69.
[39] Conradt J, Varshavskaya P. Distributed central pattern generator control for a serpentine robot. In: Proceedings of the international conference on artificial neural networks (ICANN); 2003. p. 338–41.
[40] Crespi A, Badertscher A, Guignard A, Ijspeert AJ. AmphiBot I: an amphibious snake-like robot. Robot Auton Syst 2005;50:163–75. https://doi.org/10.1016/j.robot.2004.09.015.
[41] Crespi A, Ijspeert AJ. Amphibot II: an amphibious snake robot that crawls and swims using a central pattern generator. In: Proceedings of the 9th international conference on climbing and walking robots (CLAWAR 2006); 2006. p. 19–27.
[42] Crespi A, Ijspeert AJ. Salamandra robotica: a biologically inspired amphibious robot that swims and walks. In: Artificial life models in hardware. London: Springer; 2009. p. 35–64.
[43] Crespi A, Lachat D, Pasquier A, Ijspeert AJ. Controlling swimming and crawling in a fish robot using a central pattern generator. Auton Robots 2008;25:3–13. https://doi.org/10.1007/s10514-007-9071-6.
[44] Deliagina TG, Orlovsky GN. Comparative neurobiology of postural control. Curr Opin Neurobiol 2002;12:652–7. https://doi.org/10.1016/s0959-4388(02)00376-8.
[45] Deliagina TG, Orlovsky GN, Grillner S, Wallén P. Vestibular control of swimming in lamprey. Exp Brain Res 1992;90:489–98. https://doi.org/10.1007/bf00230931.
[46] Deliagina TG, Zelenin PV, Fagerstedt P, Grillner S, Orlovsky GN. Activity of reticulospinal neurons during locomotion in the freely behaving lamprey. J Neurophysiol 2000;83:853–63. https://doi.org/10.1152/jn.2000.83.2.853.
[47] Delvolvé I, Bem T, Cabelguen JM. Epaxial and limb muscle activity during swimming and terrestrial stepping in the adult newt, pleurodeles waltl. J Neurophysiol 1997;78:638–50. https://doi.org/10.1152/jn.1997.78.2.638.
[48] Ding R, Yu J, Yang Q, Tan M. Dynamic modeling of a CPG-controlled amphibious biomimetic swimming robot. Int J Adv Robot Syst 2013;10:199. https://doi.org/10.5772/56059.
[49] Ding R, Yu J, Yang Q, Tan M, Zhang J. Robust gait control in biomimetic amphibious robot using central pattern generator. In: 2010 IEEE/RSJ international conference on intelligent robots and systems. IEEE; 2010. p. 3067–72.
[50] Donati E, Corradi F, Stefanini C, Indiveri G. A spiking implementation of the lamprey's central pattern generator in neuromorphic VLSI. In: 2014 IEEE biomedical circuits and systems conference (BioCAS) proceedings. IEEE; 2014. p. 512–5.
[51] Du S, Wu Z, Wang J, Qi S, Yu J. Design and control of a two-motor-actuated tuna-inspired robot system. IEEE Trans Syst Man Cybern Syst 2021;51:4670–80. https://doi.org/10.1109/tsmc.2019.2944786.
[52] Dubuc R, Brocard F, Antri M, Fénelon K, Gariépy JF, Smetana R, et al. Initiation of locomotion in lampreys. Brains Res Rev 2008;57:172–82. https://doi.org/10.1016/j.brainresrev.2007.07.016.
[53] Ebbeson SO. Fish neurobiology, vol. 1: brain stem and sense organs. Trends Neurosci 1983;8:178. https://doi.org/10.1016/0166-2236(85)90070-0.
[54] Eisenhart FJ, Cacciatore TW, Jr WBK. A central pattern generator underlies crawling in the medicinal Leech. J Comp Physiol A 2000;186:631–43. https://doi.org/10.1007/s003590000117.
[55] Ekeberg Ö. A combined neuronal and mechanical model of fish swimming. Biol Cybern 1993;69:363–74. https://doi.org/10.1007/BF00199436.
[56] Ekeberg Ö, Grillner S. Simulations of neuromuscular control in lamprey swimming. Philos Trans R Soc Lond B, Biol Sci 1999;354:895–902.
[57] Fagerstedt P, Ullén F. Lateral turns in the lamprey. I. Patterns of motoneuron activity. J Neurophysiol 2001;86:2246–56. https://doi.org/10.1152/jn.2001.86.5.2246.
[58] Ferrario A, Palyanov A, Koutsikou S, Li W, Soffe S, Roberts A, et al. From decision to action: detailed modeling of frog tadpoles reveals neuronal mechanisms of decision-making and reproduces unpredictable swimming movements in response to sensory signals. PLoS Comput Biol 2021;17:e1009654. https://doi.org/10.1371/journal.pcbi.1009654.
[59] Frolich LM, Biewener AA. Kinematic and electromyographic analysis of the functional role of the body axis during terrestrial and aquatic locomotion in the salamander ambystoma tigrinum. J Exp Biol 1992;162:107–30.

[60] Garcia-Rill E, Skinner R. The mesencephalic locomotor region. II. Projections to reticulospinal neurons. Brain Res 1987;411:13–20. https://doi.org/10.1016/0006-8993(87)90676-7.
[61] Getting PA. Emerging principles governing the operation of neural networks. Annu Rev Neurosci 1989;12:185–204. https://doi.org/10.1146/annurev.ne.12.030189.001153.
[62] Goulding M. Circuits controlling vertebrate locomotion: moving in a new direction. Nat Rev Neurosci 2009;10:507–18. https://doi.org/10.1038/nrn2608.
[63] Grillner S. The motor infrastructure: from ion channels to neuronal networks. Nat Rev Neurosci 2003;4:573–86. https://doi.org/10.1038/nrn1137.
[64] Grillner S. Biological pattern generation: the cellular and computational logic of networks in motion. Neuron 2006;52:751–66. https://doi.org/10.1016/j.neuron.2006.11.008.
[65] Grillner S, Ekeberg Ö, El Manira A, Lansner A, Parker D, Tegner J, et al. Intrinsic function of a neuronal network—a vertebrate central pattern generator. Brains Res Rev 1998;26:184–97.
[66] Grillner S, El Manira A. Current principles of motor control, with special reference to vertebrate locomotion. Physiol Rev 2020;100:271–320. https://doi.org/10.1152/physrev.00015.2019.
[67] Grillner S, Hellgren J, Menard A, Saitoh K, Wikstrom M. Mechanisms for selection of basic motor programs – roles for the striatum and pallidum. Trends Neurosci 2005;28:364–70. https://doi.org/10.1016/j.tins.2005.05.004.
[68] Grillner S, Kozlov A. The CPGs for limbed locomotion–facts and fiction. Int J Mol Sci 2021;22:5882. https://doi.org/10.3390/ijms22115882.
[69] Grillner S, Robertson B, Stephenson-Jones M. The evolutionary origin of the vertebrate basal ganglia and its role in action selection. J Physiol 2013;591:5425–31. https://doi.org/10.1113/jphysiol.2012.246660.
[70] Grillner S, Wallén P, Saitoh K, Kozlov A, Robertson B. Neural bases of goal-directed locomotion in vertebrates–an overview. Brains Res Rev 2008;57:2–12. https://doi.org/10.1016/j.brainresrev.2007.06.027.
[71] Kimura SAH, Sakurama K. Realization of dynamic walking and running of the quadruped using neural oscillator. Auton Robots 1999;7:247–58.
[72] Hamlet C, Fauci L, Morgan JR, Tytell ED. Proprioceptive feedback amplification restores effective locomotion in a neuromechanical model of lampreys with spinal injuries. Proc Natl Acad Sci 2023;120. https://doi.org/10.1073/pnas.2213302120.
[73] Hamlet CL, Hoffman KA, Tytell ED, Fauci LJ. The role of curvature feedback in the energetics and dynamics of lamprey swimming: a closed-loop model. PLoS Comput Biol 2018;14:e1006324. https://doi.org/10.1371/journal.pcbi.1006324.
[74] Hao Y, Cao Y, Cao Y, Huang Q, Pan G. Course control of a manta robot based on amplitude and phase differences. J Mar Sci Eng 2022;10:285. https://doi.org/10.3390/jmse10020285.
[75] Harischandra N, Knuesel J, Kozlov A, Bicanski A, Cabelguen JM, Ijspeert A, et al. Sensory feedback plays a significant role in generating walking gait and in gait transition in salamanders: a simulation study. Front Neurorobot 2011;5:3. https://doi.org/10.3389/FNBOT.2011.00003.
[76] Heliot R, Espiau B. Multisensor input for CPG-based sensory—motor coordination. IEEE Trans Robot 2008;24:191–5. https://doi.org/10.1109/tro.2008.915433.
[77] Hodgkin AL, Huxley AF. A quantitative description of membrane current and its application to conduction and excitation in nerve. J Physiol 1952;117:500–44. https://doi.org/10.1113/jphysiol.1952.sp004764.
[78] Hu Y, Liang J, Wang T. Mechatronic design and locomotion control of a robotic thunniform swimmer for fast cruising. Bioinspir Biomim 2015;10:026006. https://doi.org/10.1088/1748-3190/10/2/026006.
[79] Hu Y, Zhao W, Wang L, Jia Y. Neural-based control of modular robotic fish with multiple propulsors. In: 2008 47th IEEE conference on decision and control. IEEE; 2008. p. 5232–7.
[80] Huss M, Lansner A, Wallén P, El Manira A, Grillner S, Kotaleski JH. Roles of ionic currents in lamprey CpG neurons: a modeling study. J Neurophysiol 2007;97:2696–711. https://doi.org/10.1152/jn.00528.2006.
[81] Ijspeert AJ. A connectionist central pattern generator for the aquatic and terrestrial gaits of a simulated salamander. Biol Cybern 2001;84:331–48. https://doi.org/10.1007/s004220000211.
[82] Ijspeert AJ. Central pattern generators for locomotion control in animals and robots: a review. Neural Netw 2008;21:642–53. https://doi.org/10.1016/j.neunet.2008.03.014.
[83] Ijspeert AJ, Crespi A, Cabelguen JM. Simulation and robotics studies of salamander locomotion: applying neurobiological principles to the control of locomotion in robots. Neuroinformatics 2005;3:171–96. https://doi.org/10.1385/ni:3:3:171.
[84] Ijspeert AJ, Crespi A, Ryczko D, Cabelguen JM. From swimming to walking with a salamander robot driven by a spinal cord model. Science 2007;315:1416–20. https://doi.org/10.1126/SCIENCE.1138353.
[85] Izhikevich EM. Dynamical systems in neuroscience. MIT Press; 2007.
[86] Jahn K, Deutschländer A, Stephan T, Kalla R, Hüfner K, Wagner J, et al. Supraspinal locomotor control in quadrupeds and humans. In: Progress in brain research. Elsevier; 2008. p. 353–62.
[87] Ji P, Wang Y, Peron T, Li C, Nagler J, Du J. Structure and function in artificial, zebrafish and human neural networks. Phys Life Rev 2023;45:74–111. https://doi.org/10.1016/j.plrev.2023.04.004.
[88] Ji P, Ye J, Mu Y, Lin W, Tian Y, Hens C, et al. Signal propagation in complex networks. Phys Rep 2023;1017:1–96. https://doi.org/10.1016/j.physrep.2023.03.005.
[89] Kamali Sarvestani I, Kozlov A, Harischandra N, Grillner S, Ekeberg Ö. A computational model of visually guided locomotion in lamprey. Biol Cybern 2013;107:497–512. https://doi.org/10.1007/s00422-012-0524-4.
[90] Kamimura A, Kurokawa H, Toshida E, Tomita K, Murata S, Kokaji S. Automatic locomotion pattern generation for modular robots. In: 2003 IEEE international conference on robotics and automation (cat. no.03CH37422). IEEE; 2003. p. 714–20.
[91] Kamimura A, Kurokawa H, Yoshida E, Tomita K, Kokaji S, Murata S. Distributed adaptive locomotion by a modular robotic system, m-TRAN II. In: 2004 IEEE/RSJ international conference on intelligent robots and systems v(IROS) (IEEE cat. no. 04CH37566). IEEE; 2004. p. 2370–7.
[92] Katz HR, Hamlet CL. Mechanosensory feedback in lamprey swimming models and applications in the field of spinal cord regeneration. Integr Comp Biol 2023;63:464–73. https://doi.org/10.1093/icb/icad079.
[93] Kern S, Koumoutsakos P. Simulations of optimized anguilliform swimming. J Exp Biol 2006;209:4841–57.
[94] Kiehn O. Decoding the organization of spinal circuits that control locomotion. Nat Rev Neurosci 2016;17:224–38. https://doi.org/10.1038/nrn.2016.9.
[95] Kiemel T, Gormley KM, Guan L, Williams TL, Cohen AH. Estimating the strength and direction of functional coupling in the lamprey spinal cord. J Comput Neurosci 2003;15:233–45.
[96] Kim LU, Riecke H. Intersegmental coordination of the central pattern generator via interleaved electrical and chemical synapses in zebrafish spinal cord. J Comput Neurosci 2022;51:129–47. https://doi.org/10.1007/s10827-022-00837-5.
[97] Kimura H, Fukuoka Y, Cohen AH. Adaptive dynamic walking of a quadruped robot on natural ground based on biological concepts. Int J Robot Res 2007;26:475–90. https://doi.org/10.1177/0278364907078089.
[98] Knüsel J, Bicanski A, Ryczko D, Cabelguen JM, Ijspeert AJ. A salamander's flexible spinal network for locomotion, modeled at two levels of abstraction. Integr Comp Biol 2013;53:269–82. https://doi.org/10.1093/ICB/ICT067.
[99] Korkmaz D, Ozmen Koca G, Li G, Bal C, Ay M, Akpolat ZH. Locomotion control of a biomimetic robotic fish based on closed loop sensory feedback CPG model. J Mar Eng Technol 2021;20:125–37. https://doi.org/10.1080/20464177.2019.1638703.
[100] Kotrschal K, Staaden MV, Huber R. Fish brains: evolution and anvironmental relationships. Rev Fish Biol Fish 1998;8:373–408. https://doi.org/10.1023/a:1008839605380.

[101] Kozlov A, Huss M, Lansner A, Kotaleski JH, Grillner S. Simple cellular and network control principles govern complex patterns of motor behavior. Proc Natl Acad Sci USA 2009;106:20027–32. https://doi.org/10.1073/pnas.0906722106.
[102] Kozlov AK, Kardamakis AA, Hellgren Kotaleski J, Grillner S. Gating of steering signals through phasic modulation of reticulospinal neurons during locomotion. Proc Natl Acad Sci USA 2014;111:3591–6. https://doi.org/10.1073/pnas.1401459111.
[103] Kozlov AK, Ullén F, Fagerstedt P, Aurell E, Lansner A, Grillner S. Mechanisms for lateral turns in lamprey in response to descending unilateral commands: a modeling study. Biol Cybern 2002;86:1–14. https://doi.org/10.1007/s004220100272.
[104] Kurkin SA, Kulminskiy DD, Ponomarenko VI, Prokhorov MD, Astakhov SV, Hramov AE. Central pattern generator based on self-sustained oscillator coupled to a chain of oscillatory circuits. Chaos, Interdiscip J Nonlinear Sci 2022;32.
[105] Lachat D, Crespi A, Ijspeert AJ. BoxyBot: a swimming and crawling fish robot controlled by a central pattern generator. In: The first IEEE/RAS-EMBS international conference on biomedical robotics and biomechatronics, BioRob 2006. IEEE; 2006. p. 643–8.
[106] Lee JH, Delbruck T, Pfeiffer M. Training deep spiking neural networks using backpropagation. Front Neurosci 2016;10. https://doi.org/10.3389/fnins.2016.00508.
[107] Leiras R, Cregg JM, Kiehn O. Brainstem circuits for locomotion. Annu Rev Neurosci 2022;45:63–85. https://doi.org/10.1146/annurev-neuro-082321-025137.
[108] Li G, Zhang H, Zhang J, Hildre HP. An approach for adaptive limbless locomotion using a cpg-based reflex mechanism. J Bionics Eng 2014;11:389–99. https://doi.org/10.1016/s1672-6529(14)60052-4.
[109] Li L, Wang C, Xie G. A general CPG network and its implementation on the microcontroller. Neurocomputing 2015;167:299–305. https://doi.org/10.1016/j.neucom.2015.04.066.
[110] Liu J, Wu Z, Yu J. Design and implementation of a robotic dolphin for water quality monitoring. In: 2016 IEEE international conference on robotics and biomimetics (ROBIO). IEEE; 2016. p. 835–40.
[111] Liu Q, Wang JZ. Modeling and analysis of a new locomotion control neural networks. Biol Cybern 2018;112:345–56. https://doi.org/10.1007/s00422-018-0758-x.
[112] Liu Q, Yang H, Zhang J, Wang J. A new model of the spinal locomotor networks of a salamander and its properties. Biol Cybern 2018;112:369–85. https://doi.org/10.1007/s00422-018-0759-9.
[113] Liu Q, Zhang Y, Wang J, Yang H, Hong L. Modeling of the neural mechanism underlying the terrestrial turning of the salamander. Biol Cybern 2020;114:317–36. https://doi.org/10.1007/S00422-020-00821-1.
[114] Liu X, Onal CD, Fu J. Reinforcement learning of CPG-regulated locomotion controller for a soft snake robot. IEEE Trans Robot 2023;39:3382–401. https://doi.org/10.1109/tro.2023.3286046.
[115] Maass W. Networks of spiking neurons: the third generation of neural network models. Neural Netw 1997;10:1659–71. https://doi.org/10.1016/s0893-6080(97)00011-7.
[116] Manfredi L, Assaf T, Mintchev S, Marrazza S, Capantini L, Orofino S, et al. A bioinspired autonomous swimming robot as a tool for studying goal-directed locomotion. Biol Cybern 2013;107:513–27. https://doi.org/10.1007/s00422-013-0566-2.
[117] Manira AE, Bussières N. Calcium channel subtypes in lamprey sensory and motor neurons. J Neurophysiol 1997;78:1334–40. https://doi.org/10.1152/jn.1997.78.3.1334.
[118] Marbach D, Ijspeert A. Online optimization of modular robot locomotion. In: IEEE international conference mechatronics and automation. IEEE; 2005. p. 248–53.
[119] Marder E, Calabrese RL. Principles of rhythmic motor pattern generation. Physiol Rev 1996;76:687–717. https://doi.org/10.1152/physrev.1996.76.3.687.
[120] Martin AR, Wickelgren WO. Sensory cells in the spinal cord of the sea lamprey. J Physiol 1971;212:65–83. https://doi.org/10.1113/jphysiol.1971.sp009310.
[121] Masino MA, Fetcho JR. Fictive swimming motor patterns in wild type and mutant larval zebrafish. J Neurophysiol 2005;93:3177–88. https://doi.org/10.1152/jn.01248.2004.
[122] Matsuoka K. Sustained oscillations generated by mutually inhibiting neurons with adaptation. Biol Cybern 1985;52:367–76. https://doi.org/10.1007/bf00449593.
[123] Matsuoka K. Mechanisms of frequency and pattern control in the neural rhythm generators. Biol Cybern 1987;56:345–53. https://doi.org/10.1007/BF00319514.
[124] Matsushima T, Grillner S. Neural mechanisms of intersegmental coordination in lamprey: local excitability changes modify the phase coupling along the spinal cord. J Neurophysiol 1992;67:373–88. https://doi.org/10.1152/jn.1992.67.2.373.
[125] McKenzie DJ, Farrell AP. Fish physiology: primitive fishes. Elsevier; 2011.
[126] Shik ML, Severin FV. Control of walking and running by means of electrical stimulation of the midbrain. Biofizika 1966;11:659–66.
[127] Mnih V, Kavukcuoglu K, Silver D, Rusu AA, Veness J, Bellemare MG, et al. Human-level control through deep reinforcement learning. Nature 2015;518:529–33. https://doi.org/10.1038/nature14236.
[128] Morishita K, Takei Y, Saito K. Design of hardware-based biomimetic neural networks exhibiting oscillatory burst firing of lamprey nervous system. Trans Jpn Inst Electron Packag 2020;13. https://doi.org/10.5104/jiepeng.13.E20-007-1. E20–007–1–E20–007–4.
[129] Nakamura Y, Mori T, aki Sato M, Ishii S. Reinforcement learning for a biped robot based on a CPG-actor-critic method. Neural Netw 2007;20:723–35. https://doi.org/10.1016/j.neunet.2007.01.002.
[130] Nakao T, Ishizawa A. Development of the spinal nerves in the lamprey: I. Rohon-beard cells and interneurons. J Comp Neurol 1987;256:342–55. https://doi.org/10.1002/cne.902560304.
[131] Nielsen J, Sinkjaer T, Toft E, Kagamihara Y. Segmental reflexes and ankle joint stiffness during co-contraction of antagonistic ankle muscles in man. Exp Brain Res 1994;102. https://doi.org/10.1007/bf00227521.
[132] Nieuwenhuys R, ten Donkelaar HJ, Nicholson C. The central nervous system of vertebrates. Berlin Heidelberg: Springer; 1998.
[133] Niu X, Xu J, Ren Q, Wang Q. Locomotion learning for an anguilliform robotic fish using central pattern generator approach. IEEE Trans Ind Electron 2014;61:4780–7. https://doi.org/10.1109/TIE.2013.2288193.
[134] Northcutt R. Forebrain and midbrain organization in lizards and its phylogenetic significance. Behav Neurol Lizards 1978:11–64.
[135] Northmore DPM. The optic tectum. Elsevier; 2011.
[136] Olanow CW. The scientific basis for the current treatment of Parkinson's disease. Annu Rev Med 2004;55:41–60. https://doi.org/10.1146/annurev.med.55.091902.104422.
[137] Palyanov A, Khayrulin S, Larson SD. Three-dimensional simulation of the caenorhabditis elegans body and muscle cells in liquid and gel environments for behavioural analysis. Philos Trans R Soc Lond B, Biol Sci 2018;373:20170376. https://doi.org/10.1098/rstb.2017.0376.
[138] Parker D, Grillner S. The activity-dependent plasticity of segmental and intersegmental synaptic connections in the lamprey spinal cord. Eur J Neurosci 2000;12:2135–46. https://doi.org/10.1046/j.1460-9568.2000.00095.x.
[139] Pisarchik AN, Hramov AE. Multistability in physical and living systems: characterization and applications. Springer; 2022.
[140] Pratt J, Chew CM, Torres A, Dilworth P, Pratt G. Virtual model control: an intuitive approach for bipedal locomotion. Int J Robot Res 2001;20:129–43. https://doi.org/10.1177/02783640122067309.
[141] Previte JP, Sheils N, Hoffman KA, Kiemel T, Tytell ED. Entrainment ranges of forced phase oscillators. J Math Biol 2011;62:589–603.
[142] Ramdya P, Ijspeert AJ. The neuromechanics of animal locomotion: from biology to robotics and back. Sci Robot 2023;8. https://doi.org/10.1126/scirobotics.adg0279.

[143] Ray DL, Brocard F, Bourcier-Lucas C, Auclair F, Lafaille P, Dubuc R. Nicotinic activation of reticulospinal cells involved in the control of swimming in lampreys. Eur J Neurosci 2003;17:137–48. https://doi.org/10.1046/j.1460-9568.2003.02417.x.
[144] Ray DL, Juvin L, Boutin T, Auclair F, Dubuc R. A neuronal substrate for a state-dependent modulation of sensory inputs in the brainstem. Eur J Neurosci 2010;32:53–9. https://doi.org/10.1111/j.1460-9568.2010.07276.x.
[145] Ray DL, Juvin L, Ryczko D, Dubuc R. Supraspinal control of locomotion. In: Progress in brain research. Elsevier; 2011. p. 51–70.
[146] Davis RN. Fish neurobiology. Vol. 2, higher brain areas and functions. Trends Neurosci 1983;8:178.
[147] Righetti L, Buchli J, Ijspeert AJ. Dynamic hebbian learning in adaptive frequency oscillators. Phys D, Nonlinear Phenom 2006;216:269–81. https://doi.org/10.1016/j.physd.2006.02.009.
[148] Roberts A, Tunstall MJ, Wolf E. Properties of networks controlling locomotion and significance of voltage dependency of NMDA channels: stimulation study of rhythm generation sustained by positive feedback. J Neurophysiol 1995;73:485–95. https://doi.org/10.1152/jn.1995.73.2.485.
[149] Rovainen CM. Physiological and anatomical studies on large neurons of central nervous system of the sea lamprey (petromyzon marinus). II. Dorsal cells and giant interneurons. J Neurophysiol 1967;30:1024–42. https://doi.org/10.1152/jn.1967.30.5.1024.
[150] Rovainen CM. Synaptic interactions of identified nerve cells in the spinal cord of the sea lamprey. J Comp Neurol 1974;154:189–206. https://doi.org/10.1002/cne.901540206.
[151] Ruder L, Arber S. Brainstem circuits controlling action diversification. Annu Rev Neurosci 2019;42:485–504. https://doi.org/10.1146/annurev-neuro-070918-050201.
[152] Rueckauer B, van Gerven M. An in-silico framework for modeling optimal control of neural systems. Front Neurosci 2023;17. https://doi.org/10.3389/fnins.2023.1141884.
[153] Rulkov N, Timofeev I, Bazhenov M. Oscillations in large-scale cortical networks: map-based model. J Comput Neurosci 2004;17:203–23. https://doi.org/10.1023/b:jcns.0000037683.55688.7e.
[154] Rulkov NF. Modeling of spiking-bursting neural behavior using two-dimensional map. Phys Rev E, Stat Nonlinear Soft Matter Phys 2002;65:041922. https://doi.org/10.1103/PhysRevE.65.041922.
[155] Rybak IA, Shevtsova NA, Lafreniere-Roula M, McCrea DA. Modelling spinal circuitry involved in locomotor pattern generation: insights from deletions during fictive locomotion. J Physiol 2006;577:617–39. https://doi.org/10.1113/jphysiol.2006.118703.
[156] Ryczko D. The mesencephalic locomotor region: multiple cell types, multiple behavioral roles, and multiple implications for disease. Neuroscientist 2022;10738584221139URL. https://doi.org/10.1177/10738584221139136.
[157] Ryczko D, Auclair F, Cabelguen JM, Dubuc R. The mesencephalic locomotor region sends a bilateral glutamatergic drive to hindbrain reticulospinal neurons in a tetrapod. J Comp Neurol 2015;524:1361–83. https://doi.org/10.1002/cne.23911.
[158] Ryczko D, Charrier V, Ijspeert A, Cabelguen JM. Segmental oscillators in axial motor circuits of the salamander: distribution and bursting mechanisms. J Neurophysiol 2010;104:2677–92. https://doi.org/10.1152/jn.00479.2010.
[159] Ryczko D, Dubuc R. The multifunctional mesencephalic locomotor region. Curr Pharm Des 2013;19:4448–70. https://doi.org/10.2174/1381612811319240011.
[160] Ryczko D, Knüsel J, Crespi A, Lamarque S, Mathou A, Ijspeert AJ, et al. Flexibility of the axial central pattern generator network for locomotion in the salamander. J Neurophysiol 2015;113:1921–40. https://doi.org/10.1152/jn.00894.2014.
[161] Saitoh K, Ménard A, Grillner S. Tectal control of locomotion, steering, and eye movements in lamprey. J Neurophysiol 2007;97:3093–108. https://doi.org/10.1152/jn.00639.2006.
[162] Selzer ME. Variability in maps of identified neurons in the sea lamprey spinal cord examined by a wholemount technique. Brain Res 1979;163:181–93. https://doi.org/10.1016/0006-8993(79)90348-2.
[163] Seo K, Chung SJ, Slotine JJE. CPG-based control of a turtle-like underwater vehicle. Auton Robots 2010;28:247–69. https://doi.org/10.1007/s10514-009-9169-0.
[164] Shik ML, Severin FV, Orlovsky GN. Control of walking and running by means of electrical stimulation of the mesencephalon. Electroencephalogr Clin Neurophysiol 1969;26:549.
[165] Shilnikov AL, Rulkov NF. Origin of chaos in a two-dimensional map modeling spiking-bursting neural activity. Int J Bifurc Chaos 2003;13:3325–40. https://doi.org/10.1142/s0218127403008521.
[166] Sirota MG, Di Prisco GV, Dubuc R. Stimulation of the mesencephalic locomotor region elicits controlled swimming in semi-intact lampreys. Eur J Neurosci 2000;12:4081–92. https://doi.org/10.1046/j.1460-9568.2000.00301.x.
[167] Stein RB. A theoretical analysis of neuronal variability. Biophys J 1965;5:173–94. https://doi.org/10.1016/s0006-3495(65)86709-1.
[168] Suzuki S, Kano T, Ijspeert AJ, Ishiguro A. Decentralized control with cross-coupled sensory feedback between body and limbs in sprawling locomotion. Bioinspir Biomim 2019;14:066010. https://doi.org/10.1088/1748-3190/ab3ef6.
[169] Suzuki S, Kano T, Ijspeert AJ, Ishiguro A. Spontaneous gait transitions of sprawling quadruped locomotion by sensory-driven body-limb coordination mechanisms. Front Neurorobot 2021;15:645731. https://doi.org/10.3389/FNBOT.2021.645731.
[170] Szentagothai J, Palkovits M, Hamori J, editors. Half-centres revisited in regulatory functions of the CNS. Motion and organization principles. Pergamon Akadem Kiado; 1981.
[171] Taga G. A model of the neuro-musculo-skeletal system for anticipatory adjustment of human locomotion during obstacle avoidance. Biol Cybern 1998;78:9–17. https://doi.org/10.1007/s004220050408.
[172] Taga G, Yamaguchi Y, Shimizu H. Self-organized control of bipedal locomotion by neural oscillators in unpredictable environment. Biol Cybern 1991;65:147–59. https://doi.org/10.1007/bf00198086.
[173] Talpalar AE, Bouvier J, Borgius L, Fortin G, Pierani A, Kiehn O. Dual-mode operation of neuronal networks involved in left–right alternation. Nature 2013;500:85–8. https://doi.org/10.1038/nature12286.
[174] Tang D, Selzer ME. Projections of lamprey spinal neurons determined by the retrograde axonal transport of horseradish peroxidase. J Comp Neurol 1979;188:629–45. https://doi.org/10.1002/cne.901880408.
[175] Thandiackal R, Melo K, Paez L, Herault J, Kano T, Akiyama K, et al. Emergence of robust self-organized undulatory swimming based on local hydrodynamic force sensing. Sci Robot 2021;6:eabf6354. https://doi.org/10.1126/scirobotics.abf6354.
[176] Tong R, Feng Y, Wang J, Wu Z, Tan M, Yu J. A survey on reinforcement learning methods in bionic underwater robots. Biomim 2023;8:168. https://doi.org/10.3390/biomimetics8020168.
[177] Tong R, Qiu C, Wu Z, Wang J, Tan M, Yu J. NA-CPG: a robust and stable rhythm generator for robot motion control. Biomim Intell Robot 2022;2:100075. https://doi.org/10.1016/j.birob.2022.100075.
[178] Traven HG, Brodin L, Lansner A, Ekeberg O, Wallen P, Grillner S. Computer simulations of NMDA and non-NMDA receptor-mediated synaptic drive: sensory and supraspinal modulation of neurons and small networks. J Neurophysiol 1993;70:695–709. https://doi.org/10.1152/jn.1993.70.2.695.
[179] Tsai CW, Lin CL, Huang CH. Microbrushless dc motor control design based on real-coded structural genetic algorithm. IEEE/ASME Trans Mechatron 2010;16:151–9.
[180] Turnbull J. The welfare of fish - edited by TS kristiansen. Kristiansen TS, Ferno A, Pavlidis MA, van de Vis H, editors. Animal welfare, vol. 30. Heidelberg, Germany: Springer Nature; 2020. p. 229–30.
[181] Tytell ED, Carr JA, Danos N, Wagenbach C, Sullivan CM, Kiemel T, et al. Body stiffness and damping depend sensitively on the timing of muscle activation in lampreys. Integr Comp Biol 2018. https://doi.org/10.1093/icb/icy042.

[182] Tytell ED, Hsu CY, Williams TL, Cohen AH, Fauci LJ. Interactions between internal forces, body stiffness, and fluid environment in a neuromechanical model of lamprey swimming. Proc Natl Acad Sci USA 2010;107:19832–7. https://doi.org/10.1073/pnas.1011564107.
[183] Tytell ED, Leftwich MC, Hsu CY, Griffith BE, Cohen AH, Smits AJ, et al. Role of body stiffness in undulatory swimming: insights from robotic and computational models. Phys Rev Fluids 2016;1. https://doi.org/10.1103/physrevfluids.1.073202.
[184] Verdaasdonk B, Koopman H, Helm FVD. Energy efficient and robust rhythmic limb movement by central pattern generators. Neural Netw 2006;19:388–400. https://doi.org/10.1016/j.neunet.2005.09.003.
[185] Verma S, Shen D, Xu JX. Motion control of robotic fish under dynamic environmental conditions using adaptive control approach. IEEE J Ocean Eng 2018;43:381–90. https://doi.org/10.1109/joe.2017.2758158.
[186] Vukobratović M, Borovac B. ZERO-MOMENT POINT — THIRTY FIVE YEARS OF ITS LIFE. Int J Humanoid Robot 2004;01:157–73. https://doi.org/10.1142/s0219843604000083.
[187] Wallen P, Ekeberg O, Lansner A, Brodin L, Traven H, Grillner S. A computer-based model for realistic simulations of neural networks. II. The segmental network generating locomotor rhythmicity in the lamprey. J Neurophysiol 1992;68:1939–50. https://doi.org/10.1152/jn.1992.68.6.1939.
[188] Wang C, Xie G, Wang L, Cao M. Cpg-based locomotion control of a robotic fish: using linear oscillators and reducing control parameters via pso. Int J Innov Comput Inf Control 2011;7:4237–49.
[189] Wang J, Hu C, Zhu Y. CPG-based hierarchical locomotion control for modular quadrupedal robots using deep reinforcement learning. IEEE Robot Autom Lett 2021;6:7193–200. https://doi.org/10.1109/lra.2021.3092647.
[190] Wang M, Dong H, Li X, Zhang Y, Yu J. Control and optimization of a bionic robotic fish through a combination of CPG model and PSO. Neurocomputing 2019;337:144–52. https://doi.org/10.1016/J.NEUCOM.2019.01.062.
[191] Wang M, Yu J, Tan M, Zhang J. Multimodal swimming control of a robotic fish with pectoral fins using a CPG network. Chin Sci Bull 2012;57:1209–16. https://doi.org/10.1007/s11434-012-5005-6.
[192] Wang W, Gu D, Xie G. Autonomous optimization of swimming gait in a fish robot with multiple onboard sensors. IEEE Trans Syst Man Cybern Syst 2019;49:891–903. https://doi.org/10.1109/tsmc.2017.2683524.
[193] Wang W, Guo J, Wang Z, Xie G. Neural controller for swimming modes and gait transition on an ostraciiform fish robot. In: 2013 IEEE/ASME international conference on advanced intelligent mechatronics. IEEE; 2013. p. 1564–9.
[194] Wang W, Xie G. CPG-based locomotion controller design for a boxfish-like robot. Int J Adv Robot Syst 2014;11:87. https://doi.org/10.5772/58564.
[195] Wannier T, Deliagina TG, Orlovsky GN, Grillner S. Differential effects of the reticulospinal system on locomotion in lamprey. J Neurophysiol 1998;80:103–12. https://doi.org/10.1152/jn.1998.80.1.103.
[196] Westphal A, Rulkov NF, Ayers J, Brady D, Hunt M. Controlling a lamprey-based robot with an electronic nervous system. Smart Struct Syst 2011;8:39–52. https://doi.org/10.12989/sss.2011.8.1.039.
[197] Wu X, Ma S. Neurally controlled steering for collision-free behavior of a snake robot. IEEE Trans Control Syst Technol 2013;21:2443–9. https://doi.org/10.1109/tcst.2012.2237519.
[198] Wu Z, Yu J, Su Z, Tan M, Li Z. Towards an esox lucius inspired multimodal robotic fish. Sci China Inf Sci 2015;58:1–13. https://doi.org/10.1007/s11432-014-5202-9.
[199] Wu Z, Yu J, Tan M, Zhang J. Kinematic comparison of forward and backward swimming and maneuvering in a self-propelled sub-carangiform robotic fish. J Bionics Eng 2014;11:199–212. https://doi.org/10.1016/s1672-6529(14)60037-8.
[200] Xie F, Li Z, Ding Y, Zhong Y, Du R. An experimental study on the fish body flapping patterns by using a biomimetic robot fish. IEEE Robot Autom Lett 2020;5:64–71. https://doi.org/10.1109/lra.2019.2941827.
[201] Xie F, Zhong Y, Du R, Li Z. Central pattern generator (CPG) control of a biomimetic robot fish for multimodal swimming. J Bionics Eng 2019;16:222–34. https://doi.org/10.1007/S42235-019-0019-2.
[202] Yang Y, Wang J, Wu Z, Yu J. Fault-tolerant control of a CPG-governed robotic fish. Engineering 2018;4:861–8. https://doi.org/10.1016/j.eng.2018.09.011.
[203] Yao G, Liang J, Wang T, Yang X, Shen Q, Zhang Y, et al. Development of a turtle-like underwater vehicle using central pattern generator. In: 2013 IEEE international conference on robotics and biomimetics (ROBIO). IEEE; 2013. p. 44–9.
[204] Yin XY, Jia LC, Wang C, Xie GM. The effect of waist twisting on walking speed of an amphibious salamander like robot. Acta Mech Sin 2015;32:546–50. https://doi.org/10.1007/s10409-015-0532-4.
[205] Youssef I, Mutlu M, Bayat B, Crespi A, Hauser S, Conradt J, et al. A neuro-inspired computational model for a visually guided robotic lamprey using frame and event based cameras. IEEE Robot Autom Lett 2020;5:2395–402. https://doi.org/10.1109/LRA.2020.2972839.
[206] Yu J, Chen S, Wu Z, Wang W. On a miniature free-swimming robotic fish with multiple sensors. Int J Adv Robot Syst 2016;13:62. https://doi.org/10.5772/62887.
[207] Yu J, Ding R, Yang Q, Tan M, Zhang J. Amphibious pattern design of a robotic fish with wheel-propeller-fin mechanisms. J Field Robot 2013;30:702–16. https://doi.org/10.1002/rob.21470.
[208] Yu J, Tan M, Chen J, Zhang J. A survey on CPG-inspired control models and system implementation. IEEE Trans Neural Netw Learn Syst 2014;25:441–56. https://doi.org/10.1109/tnnls.2013.2280596.
[209] Yu J, Wang C, Xie G. Coordination of multiple robotic fish with applications to underwater robot competition. IEEE Trans Ind Electron 2016;63:1280–8. https://doi.org/10.1109/tie.2015.2425359.
[210] Yu J, Wang K, Tan M, Zhang J. Design and control of an embedded vision guided robotic fish with multiple control surfaces. Sci World J 2014;2014:1–13. https://doi.org/10.1155/2014/631296.
[211] Yu J, Wang M, Su Z, Tan M, Zhang J. Dynamic modeling of a CPG-governed multijoint robotic fish. Adv Robot 2013;27:275–85. https://doi.org/10.1080/01691864.2013.755279.
[212] Yu J, Wang M, Tan M, Zhang J. Three-dimensional swimming. IEEE Robot Autom Mag 2011;18:47–58. https://doi.org/10.1109/mra.2011.942998.
[213] Yu J, Wu Z, Wang M, Tan M. CPG network optimization for a biomimetic robotic fish via PSO. IEEE Trans Neural Netw Learn Syst 2016;27:1962–8. https://doi.org/10.1109/tnnls.2015.2459913.
[214] Zhang D, Pan G, Cao Y, Huang Q, Cao Y. A novel integrated gliding and flapping propulsion biomimetic manta-ray robot. J Mar Sci Eng 2022;10:924. https://doi.org/10.3390/jmse10070924.
[215] Zhang DB, Hu DW, Shen LC, Xie HB. A bionic neural network for fish-robot locomotion. J Bionics Eng 2006;3:187–94. https://doi.org/10.1016/S1672-6529(07)60002-X.
[216] Zhang S, Qian Y, Liao P, Qin F, Yang J. Design and control of an agile robotic fish with integrative biomimetic mechanisms. IEEE/ASME Trans Mechatron 2016;21:1846–57. https://doi.org/10.1109/TMECH.2016.2555703.
[217] Zhang T, Tian R, Wang C, Xie G. Path-following control of fish-like robots: a deep reinforcement learning approach. IFAC-PapersOnLine 2020;53:8163–8. https://doi.org/10.1016/j.ifacol.2020.12.2306.
[218] Zhang T, Wang R, Wang Y, Cheng L, Wang S, Tan M. Design and locomotion control of a dactylopteridae-inspired biomimetic underwater vehicle with hybrid propulsion. IEEE Trans Autom Sci Eng 2022;19:2054–66. https://doi.org/10.1109/tase.2021.3070117.
[219] Zhao W, Hu Y, Wang L, Zhang L. Design and CPG-based control of biomimetic robotic fish. IET Control Theory Appl 2009;3:281–93. https://doi.org/10.1049/iet-cta:20070204.
[220] Zhong B, Zhang S, Xu M, Zhou Y, Fang T, Li W. On a CPG-based hexapod robot: AmphiHex-II with variable stiffness legs. IEEE/ASME Trans Mechatron 2018;23:542–51. https://doi.org/10.1109/tmech.2018.2800776.

[221] Zhou C, Low KH. Design and locomotion control of a biomimetic underwater vehicle with fin propulsion. IEEE/ASME Trans Mechatron 2012;17:25–35. https://doi.org/10.1109/tmech.2011.2175004.
[222] Zhou C, Low KH. On-line optimization of biomimetic undulatory swimming by an experiment-based approach. J Bionics Eng 2014;11:213–25. https://doi.org/10.1016/s1672-6529(14)60042-1.